People's Democratic Republic of Algeria
Ministry of Higher Education and Scientific Research
Echahid Hamma Lakhdar University of El-Oued
Faculty of Exact Sciences
Department of Chemistry

Master thesis

in chemistry

Speciality *Organic chemistry*

Presented by
Athar BAHRI
Souad DARRADJI
Maroua NEDJIMA

Title

Synthesis, characterization and application of hydroxyapatite in dental resin

Publicly defended on.15/06/2022 before the jury composed of:

Dr. H. DEBBECHE	University of El-Oued	President
Pr. M. DEHAMCHIA	University of El-Oued	Examiner
Dr. S.BAYOU	University of El-Oued	Supervisor

2021/2022

People's Democratic Republic of Algeria
Ministry of Higher Education and Scientific Research
Echahid Hamma Lakhdar University of El-Oued
Faculty of Exact Sciences
Department of Chemistry

Master thesis

in chemistry

Speciality *Organic chemistry*

Presented by
Athar BAHRI
Souad DARRADJI
Maroua NEDJIMA

Title

Synthesis, characterization and application of hydroxyapatite in dental resin

Publicly defended on.15/06/2022 before the jury composed of:

Dr. H. DEBBECHE	University of El-Oued	President
Pr. M. DEHAMCHIA	University of El-Oued	Examiner
Dr. S.BAYOU	University of El-Oued	Supervisor

2021/2022

DEDICATION

I dedicate the thesis to : The sake of Allah, my Creator and my Master.
My great teacher and messenger, Mohammed (May Allah bless and grant him). My amazing mother and My great dad , who never stop giving of themselves in countless ways.
My dearest sister and my beloved brothers.
My dear grandmothers and the pure souls of my grandfathers.
To all who supported me in my academic career.

ATHAR

I dedicate this thesis:
To my beloved father and my beautiful mother, you have been the best supporters throughout my academic career and never failed to give me financial and moral support .
To the people closest to myself: my wonderful sisters and brothers, particularly my dearest brother ***Walid*** who stayed by my side while I was writing this thesis ... Not for anything but only to play with my laptop.
To my family, friends and everyone who contributed to the enrichment of this work from near or far.
To everyone from whom I received advice and support .

MAROUA

To the one who encouraged me to persevere all my life ,to the most prominent man in my life
(my dear father)
To whom I rise, and upon whom I rest, to giving heart
(my beloved mother)
To those who made an effort to help me, they were the best support
(dear brothers)
To my family, to my friends and colleagues. . . ..
To everyone who contributed even a letter to my academic life. . . ..
To all of them I dedicate this work, I ask God Almighty to accept sincerely.

SOUAD

Acknowlegments

In the Name of Allah, the Most Merciful, the Most Compassionate all praise be to Allah, the Lord of the worlds; and prayers and peace be upon Mohamed His servant and messenger. First and foremost, we must acknowledge our limitless thanks to Allah, the Ever-Magnificent; the Ever-Thankful, for His help and bless. We would like to express our sincere thanks to our supervisor **Dr. Bayou** for his help, follow-up, support, encouragement and valuable advice for making this thesis despite his duties and interests.

We extend our sincere thanks and appreciations to **Dr. DEBBECHE** and **Pr. DEHAMCHIA**, for their eagerness to evaluate this work. We would like to thank **Dr. Mimouni** for his help in the final results, **Dr. Guedda** , **Ms Karima** and **Ms. Djihad** for their help during practical work for good results.

Sincere thanks and appreciation to the PhD students who have never been stingy with advice: **Ichrak, Chaima, Amina, Abir, Siham and Fath Eddin**. Last but not least, deepest thanks go to all people who took part in making this thesis real.

Abbreviation

Symbole	Designation
Bis-GMA	bisphenol A-glycidyl methacrylate or 2,2-bis[4(2-hydroxy-3-methacryloxy-propyloxy)- phenyl] propane
BP	benzophenone
BPO	benzoyl peroxide
CQ	camphorquinone
EGDMA	Ethylene Glycol DiMethAcrylate
DEGMA	DiEthylene Glycol diMethAcrylate
FTIR	Fourier Transform Infrared
HAp	hydroxyapatite $Ca_{10}(PO_4)_6(OH)_2$
HOMO	highest occupied molecular orbital
LED	light-emitting diode
LUMO	lowest unoccupied molecular orbital
MMA	Methyl MethAcrylate
Mo	monomer concentration
N-HAp	natural hydroxyapatite
p-HAp-b-(25°C)	the HAp obtained by precipitation from brown eggshells in (25°C)
p-HAp-b-(900°C)	the HAp obtained by precipitation from brown eggshells after heat treatment in 900°C
p-HAp-w-(25°C)	the HAp obtained by precipitation from white eggshells in (25°C)
p-HAp-w-(900°C)	the HAp obtained by precipitation from white eggshells after heat treatment in 900°C
PPD	1-phenyl-1,2 propanodione
PQ	phenanthrenequinone
T-HAp 0h	the HAp obtained by hydrothermal method in (25°C)
T-HAp 5h	the HAp obtained by hydrothermal method in teflon autoclave for 5h (150°C)
TEGDMA	TriEthylene Glycol DiMethAcrylate
TMPTMA	TriMethylPropaneTriMethAcrylate 2,2-bis (prop-2-enoyloxymethyl) butyl prop-2-enoate
TPO	trimethylbenzoyl-diphenylphosphine oxide
UDMA	urethane dimethacrylate
A	photo-initiator concentration

A_0	the initial absorbance of the methacrylate groups before photopolymerization
A_t	the absorbance at time t of the methacrylate groups after photopolymerization.
DC_t	the degree of conversion of methacrylic double bonds
I_0	incident radiation intensity
K_p	propagation rate constant
K_t	termination rate constant
ϕ	initiation quantum yield
ε	molar extinction coefficient
CaO	calcium oxide
$Ca(OH)_2$	Calcium hydroxide
H_3PO_4	phosphoric acid
$CaCl_2$	Calcium chloride
NH_4OH	Ammonium hydroxide
NH_4Cl	Ammonium chloride

List of Figures

I.1 Tooth structure. 2
I.2 Stages of tooth decay 3
I.3 An example for amalgam restoration 3
I.4 An example for silicate cement restoration. 4
I.5 An example for dental composites restoration 4
I.6 Schematic of dental composite and location of components. 4
I.7 Synthesis of bisphenol A glycidyl dimethacrylate Bis-GMA 5
I.8 Chemical Structure of UDMA 6
I.9 Branched monomer 6
I.10 Hyper-branched monomer 6
I.11 Different types of viscosity controller monomer 7
I.12 Structure of photo-initiators 7
I.13 Mechanism of decomposition of benzoyl peroxide in the presence of a tertiary amine 8
I.14 Diagram interface matrix – load 9
I.15 Examples of light-curing methacrylate silanes. 9
I.16 Chemically activated composite resin (chemical polymerization) 9
I.17 Light activated composite resin (photopolymerization) 10
I.18 Classification of dental composites on the basis of particle size and structure. . . . 10

II.1 (a) Atomic formula of HAp. (b) Representation along the (c) axis. 15
II.2 Synthesis of precipitation. 17
II.3 The manufacture of hydroxyapatite by the sol-gel method. 17
II.4 Hydroxyapatite synthesis using hydrothermal method 18
II.5 Manufacture of hydroxyapatite by dry method 18
II.6 Manufacture of hydroxyapatite from biological sources 19

III.1 Formation of three-dimensional network by photo-polymerization 29
III.2 Diagram of the photo-polymerization process 29
III.3 Some examples of cationic photo-initiators 30
III.4 Some examples of radical initiators type 1 32
III.5 Benzophenone activation principle 32
III.6 Examples of type two radical photo-initiators 33
III.7 The different lamp used in dental offices. 34

IV.1 Chicken brown eggshell anatomy 38
IV.2 Preparation of HAp from natural source 39

IV.3 Protocol for precipitation method 40
IV.4 Scheme for hydro-thermal method 41
IV.5 FT-IR spectra for N-HAp 41
IV.6 FT-IR spectra for p-HAp-w-(25°C) and p-HAp-w-(900°C). 42
IV.7 FT-IR spectra for p-HAp-b-(25°C) and p-HAp-b-(900°C) 43
IV.8 FT-IR spectra for T-HAp 0h and T-HAp 5h. 44
IV.9 XRD patterns of p-HAp-w-(900°C), p-HAp-b-(900°C) and T-HAp 5h powders. . . 46
IV.10 XRD pattern of pure hydroxyapatite 46

V.1 Chemical structure of monomers and organic phase initiation system (resin). 50
V.2 Schematic representation of a sample positioned in contact with the crystal of the ATR-FTIR device. 51
V.3 FT-IR spectrum for C=C and C=O group before and after photo-polymerization. . . 52
V.4 The evolution of the DC of the methacrylate of resin (TMPTMA/DEGDMA) group as a function of the polymerization time 53
V.5 Evolution of the polymerization rate as a function of resin time (TMPTMA/DEGDMA). 54
V.6 DC variation of composite different contents of hydroxyapatite (p-HAp-w-(900°C).) from 0 to 50%. 55
V.7 DC variation of the composite at different hydroxyapatite (T-HAp 5h)contents from 0 to 50%. 56
V.8 Comparison of the two types of composites P-HAp-w-(900°C) and T-HAp 5h. . . . 56

List of Tables

II.1 Comparison of hydroxyapatite obtained by different methods. 20

IV.1 Reagents and solvents used in this synthesis 38
IV.2 FT-IR spectra characteristic peak of HAp from natural source 42
IV.3 FT-IR spectra characteristic peak of p-HAp-w-(25°C) and p-HAp-w-(900°C). . . . 43
IV.4 FT-IR spectra characteristic peak of p-HAp-b-(25°C) and p-HAp-b-(900°C). 44
IV.5 FT-IR spectra characteristic peaks of T-HAp 0h and T-HAp 5h. 45
IV.6 Comparison of the best resulting samples 45
IV.7 Crystallite size and parameters of the retinal structure of p-HAp-w-(900°C), p-HAp-b-(900°C) and T-HAp 5h 46

V.1 Quantities and physical properties of resins used in the composite.(M=molar mass, $\mu = viscosity$) 50
V.2 The values of DC at each instant t 53
V.3 DC variation of composite different contents of hydroxyapatite from 0 to 50%. . . . 55

Contents

List of Figures v

List of Tables vii

General introduction xi

I DENTAL RESIN 1

I.1 Introduction . . . 2
I.2 Structure of tooth . . . 2
I.3 Dental caries . . . 3
I.4 Dental restorative material . . . 3
I.5 Resin composites . . . 4
I.6 Composition of dental resins . . . 5
Resin matrix (organic phase) . . . 5
Filler particles (inorganic phase) . . . 8
Coupling agents . . . 8
Polymerization process of composite resin . . . 9
I.7 Classification of dental composites . . . 10
I.8 Properties of resin composite . . . 11
Polymerization shrinkage . . . 11
Water absorption . . . 11
I.9 Conclusion . . . 11
Bibliography . . . 12

II HYDROXYAPATITE 14

II.1 Introduction . . . 15
II.2 Structure and chemical formula . . . 15
II.2.1 Crystal formula . . . 15
II.3 Preparation methods . . . 16
II.3.1 Precipitation . . . 16
II.3.2 Sol - gel method . . . 17
II.3.3 Hydrothermal manufacturing . . . 17
II.3.4 Dry method . . . 18
II.3.5 The liquid phase method . . . 18
II.3.6 Manufacturing from industrial resources . . . 18
II.3.7 Microwave method . . . 19

II.4 Effect of different manufacturing methods on the properties of hydroxyapatite . . . 19
II.5 Hydroxyapatite Applications: . . . 23
II.6 Conclusion . . . 23
Bibliography . . . 24

III PHOTO-POLYMERIZATION 26
III.1 Introduction . . . 27
III.2 Polymerization . . . 27
III.2.1 Definition . . . 27
III.2.2 Polymerization in addition . . . 27
III.2.3 Condensation polymerization . . . 28
III.3 Photo-polymerization . . . 28
III.3.1 Definition . . . 28
III.3.2 Principle . . . 29
III.3.3 Photo-polymerization mechanism . . . 29
III.3.4 Photo-polymerization reactions . . . 30
III.3.5 Factors influencing the efficiency of polymerization . . . 34
III.4 Light sources used in dentistry : . . . 34
III.5 Degree of conversion: . . . 35
III.6 Conclusion . . . 35
Bibliography . . . 36

IV Synthesis and characterization of hydroxyapatite (HAp) 37
IV.1 Introduction . . . 38
IV.2 The products' use . . . 38
IV.3 Synthesis of hydroxyapatite . . . 38
IV.3.1 Preparation of HAp from natural source: . . . 38
IV.3.2 Synthesis of HAp by precipitation: . . . 39
IV.4 HAp synthesis by hydro-thermal method . . . 40
IV.5 Characterization of hydroxyapatite . . . 41
IV.5.1 Fourier Transform Infrared (FTIR) analyses . . . 41
IV.5.2 X-ray diffraction analyses . . . 45
IV.6 Conclusion . . . 46

V Photo-polymerization of dental composites filled with hydroxyapatite 49
V.1 Introduction . . . 50
V.2 The products' use . . . 50
V.3 Preparation of experimental composites . . . 51
V.4 Method for monitoring the light-curing reaction . . . 51
V.4.1 Analytical technique . . . 51

V.4.2 Preparation of samples analyzed by IR 51
V.4.3 Calculation of degree of conversion 52
V.4.4 Polymerization speed 53
V.5 Effect of time on the degree of conversion: 53
V.6 Effect of filler ratio on the degree of conversion 54
V.7 Effect of the filler type on the degree of conversion 56
V.8 Conclusion 57

General conclusion **58**

Annex **60**

GENERAL INTRODUCTION

The technological developments of composite materials are mainly influenced by the tendency to create materials indispensable to our daily, ecological, and environmentally friendly lives. These tend to include, in particular, the synthesis of new polymeric materials and the use of light in industrial processes[1]. Dental composites replaced mineral amalgams, which contained mercury. This material, when affected by body temperature, evaporates and goes directly to the brain, causing cancer [2].

A dental composite is an aesthetic, heterogeneous material composed of an organic matrix, a mineral or organic reinforcement in the presence of coupling agents, and various additives (initiators, accelerators, etc.). In this thesis, hydroxyapatite has been prepared by 2 methods (precipitation and hydrothermal method), and it is found in nature in bovine bone and fish scales. HAp with the natural femur bone, has been used to compare synthesis.

In this thesis, we will prepare a dental composite according to HAp, which has been prepared, and will study its physical properties by resuming DC and finding a better ratio for these composites.

This thesis has five chapters:

The first chapter talks about dental resin; it studies the structure of teeth, the different stages of dental caries, and the history of dental restorative materials, then it studies the resin composite and its composition, its classifications, and properties.

The second chapter talks about HAp, where it explains the structure and chemical formula of HAp, the different preparation methods: precipitation, sol-gel ... It also studies the effects of different manufacturing methods on the properties of hydroxyapatite and finally takes its application.

The third chapter talks about photopolymerization. It requires the general introduction of polymerization and its reaction. After that, it talks about photo-polymerization specifically, its different reactions, and the factors influencing the efficiency of polymerization. In order for the polymerization process to occur, it must have a light source that has an effect on the polymers. Then it will be able to calculate the degree of conversion.

The fourth chapter studies the synthesis and characterization of HAp which has been prepared from a natural source namely chicken eggshells. It is prepared from chemicals, and is taken from nature. The resulting samples were subjected to IR and XDR analyses to identify the results. The fifth chapter talks about photo-polymerization of composite resin, which takes the resulting samples from chapter four and mixes them with the matrix to make dental resin and calculates the degree of conversion.

Bibliography

[1] I. A. Mjör, J. E. Moorhead, and J. E. Dahl, Reasons for replacement of restorations in permanent teeth in general dental practice. International dental journal, 50(6), 361-366, 2000.

[2] S. Bayou. Etude physico-chimique de formulations dentaires chargées. PhD thesis, University of Houari Boumediene Alger, 2013.

CHAPTER I

DENTAL RESIN

I.1 Introduction

In this chapter, we will see the composition of tooth , the types of dental caries and it effect on tooth. then we will introduce dental restorative material (amalgam, silicate cement and dental composite). In this chapter, the focus will be on resin composite, it composition and properties.

I.2 Structure of tooth

A tooth is generally divided into two parts: dental crown (which is the upper visible part of the tooth) and the root (the lower part of it) (**Figure I.1 [1]**). The tooth is generally consist of:

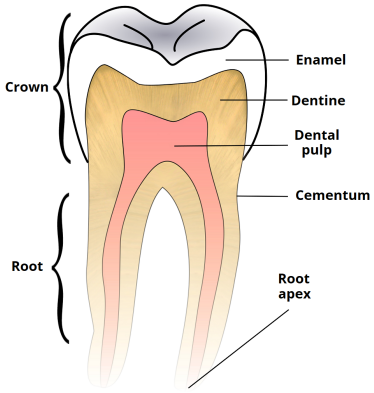

Figure I.1: Tooth structure.

Enamel: which covers dental crowns, is the thinnest tissue. Enamel is essentially made up of realized hydroxyapatite ($Ca_{10}(PO_4)_6(OH)_2$) crystals in the body (90 ٪), and to a lesser extent carbon, fluorine and minimal amounts (less than 1٪) of other ions such as potassium, nitrate etc.

Dentin: is the calcified tissue that occupies, quantitatively, the largest volume of the tooth. The dentin is covered at the coronal level by the enamel which protects it from the external environment and at the root level by the cementum where the fibers of the periodontium are anchored. [20]

The pulp: occupies the central area of the tooth. It is a connective tissue whose cellular, vascular (blood vessels) and nervous (nerves) structural elements ensure the vitality of the tooth. The pulp is surrounded, coronally and radicularly, by mineralized dentin. The nerves and blood vessels of the pulp communicate with the rest of the vascular and nervous system through the openings located at the ends of the roots[20].

Cementum: is composed of small crystals of hydroxyapatite, fluorine and magnesium and covers the root surface of the teeth. It participates in the attachment mechanism of the tooth in the alveolar bone (bone surrounding the tooth and lining the dental socket). The fibers of the periodontal ligament are inserted on the outer surface of the cementum[20].

I.3 Dental caries

Tooth decay is a very common disease that is caused by the accumulation of bacteria, where the enamel is affected (the first stage of decay), then the dentin is perforated (the second stage; the teeth become sensitive to cold and heat) and the last stage is the arrival of bacteria to the pulp of the teeth (inflames) **FigureI.2[2]**, which causes pain sharp to connect the core to the neural network. If left untreated, tooth decay can cause Gargarene[4].

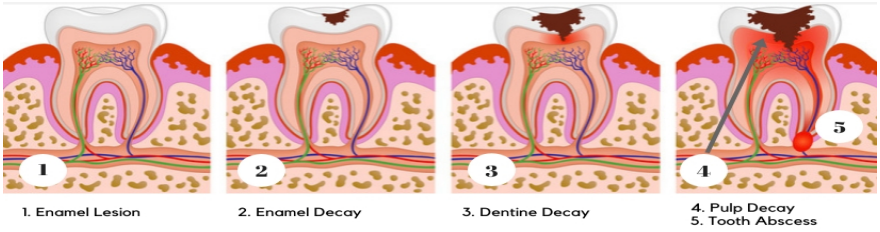

Figure I.2: Stages of tooth decay

I.4 Dental restorative material

In spite of the success in the prevention of dental caries, teeth in need of restoration still occur. In the case of dental treatment, diseased tissue is removed and teeth restored with appropriate material(s) [15].

At the beginning of the 19th century, the first biological material for dental restoration appeared amalgam (an alloy consisting of tin, silver, copper and mercury). But it was later discovered that it is harmful to human health **Figure I.3[4]**. After another bio-material appeared: the silicate cement

Figure I.3: An example for amalgam restoration

or groove sealing which is a mixture of acids, the latter also created a problem in the dental gum because of its high acidity **figure I.4[4]**.

Figure I.4: An example for silicate cement restoration.

All these defects have led researchers to develop new materials less toxic and resistant to aggressive stress in the oral environment, that they are the dental composites **figure I.5[4, 15]**.

Figure I.5: An example for dental composites restoration

I.5 Resin composites

In these days amalgam is increasingly being replaced by aesthetic restorative materials, whose color mimics that of natural tooth. Composite resins that can be cured using visible light are the most widely used for direct aesthetic restoration. The main composition of composite is an organic resin matrix, which provides sufficient fluidity for easy application of the composite , and allows polymerization for rapid setting of the composite resin, the inorganic filler, which gives rigidity, hardness and strength to the filling. Also, there is coupling agent [9, 24](**Figure I.6[7]**).

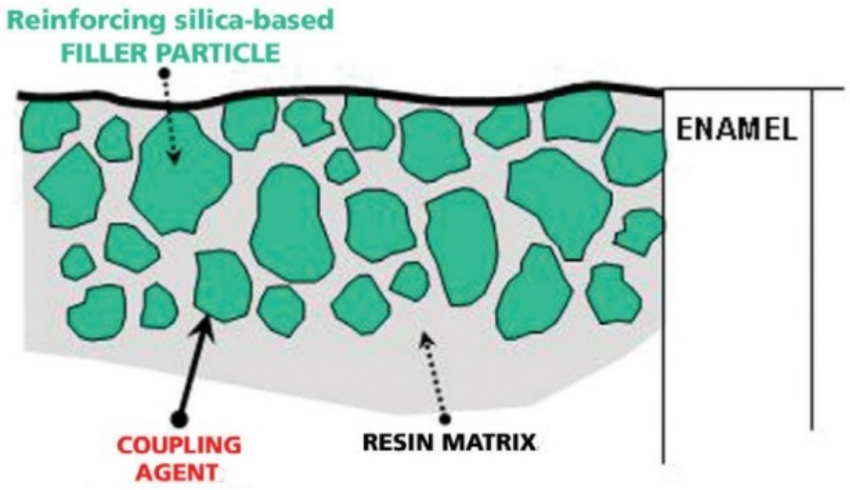

Figure I.6: Schematic of dental composite and location of components.

I.6 Composition of dental resins

Resin matrix (organic phase)

The organic phase is 25 to 50٪from the volume of resin composites. The organic matrix is typically based on dimethacrylate resins, while fillers vary depending on size, shape,and morphology, each offering different properties depending on the properties that the dental resin must provide[19].It is divided to three elements: monomers,diluents (viscosity controllers), initiators, accelerators and inhibitors.

Monomers or oligomers

It is the chemically active component of the composite. This is a fluid monomer that is converted into a rigid polymer by a reaction of polymerization [6]. These are all «R - di methacrylate» monomers, thus making all composite resins compatible with each other and with adhesives [17]. The most commonly used monomeric matrices in composite resin distribution today are 2,2-bis[4(2-hydroxy-3-methacryloxy-propyloxy)- phenyl] propane (Bis-GMA) and urethane dimethacrylate (UDMA), Both monomers have reactive carbon double bond at each end of monomer chain which will increase during polymerization [18].

Bis-GMA(bisphenol A-glycidyl methacrylate) Bis-GMA (molecular weight of 512.6 $g.mol^{-1}$) is a highly viscous (1200 Pa s) monomer because of its bulky chemical structure, hydroxyl moieties that can participate in hydrogen bonding, and the aromatic groups that can participate in $\pi = \pi$ bonding[10]. Bis-GMA can be prepared according to the reaction in **figure I.7[22]**.

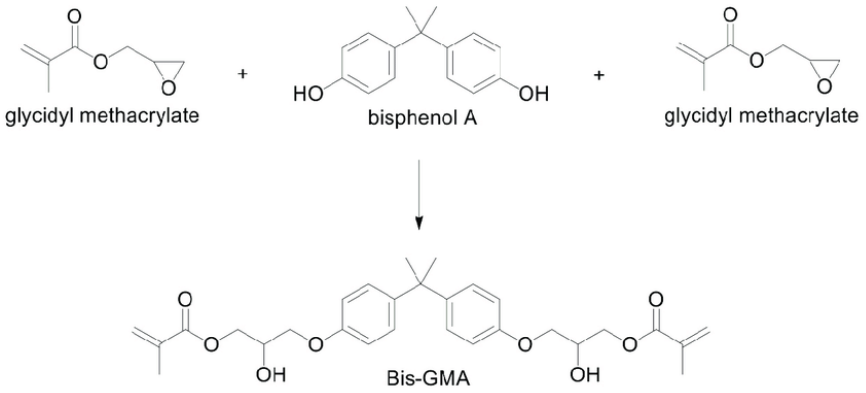

Figure I.7: Synthesis of bisphenol A glycidyl dimethacrylate Bis-GMA

Urethane dimethacrylate (UDMA) Dimethacrylate urethane is another type of high molecular weight and more flexible monomer used in the matrix of dental composites. This compound contains urethane groups characterized by the presence of NH groups which can form hydrogen bonds (**figure I.8**). Other studies have been conducted to develop other types of oligomers. They

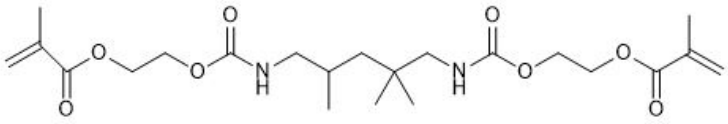

Figure I.8: Chemical Structure of UDMA

find many derivatives of methacrylates: connected monomers having new geometries and hyper-connected monomers or dendrimers (**FiguresI.9 and I.10)[4]**. This type of high viscosity material

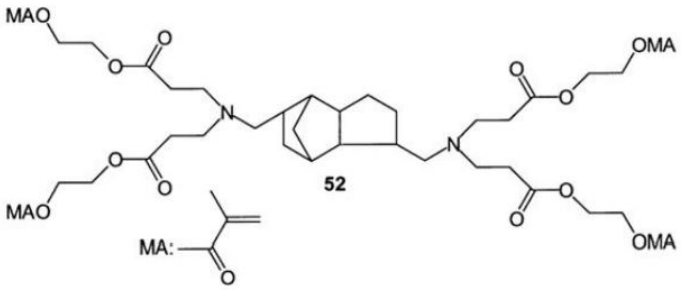

Figure I.9: Branched monomer

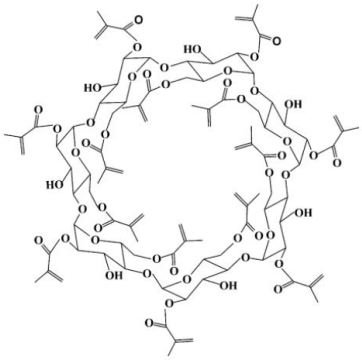

Figure I.10: Hyper-branched monomer

needs compounds that make it less viscous and easier to deal with, because of that it needs to **diluents or viscosity controllers**.

diluents (viscosity controllers)

The high molecular weight of the monomers Bis GMA and diurethane dimethyacrylate make them particularly viscous. To increase the mechanical properties it is necessary to add loads and for this to associate less viscous monomers. These are viscosity controllers or thinners.

- MMA: Methyl MethAcrylate,
- EGDMA: Ethylene Glycol DiMethAcrylate,
- DEGMA: DiEthylene Glycol diMethAcrylate,
- TEGDMA: TriEthylene Glycol DiMethAcrylate.

The manufacturer, depending on the viscosity of the expected material, will vary the content by diluting, and change its physical properties. The diluent increases the setting retraction [9]

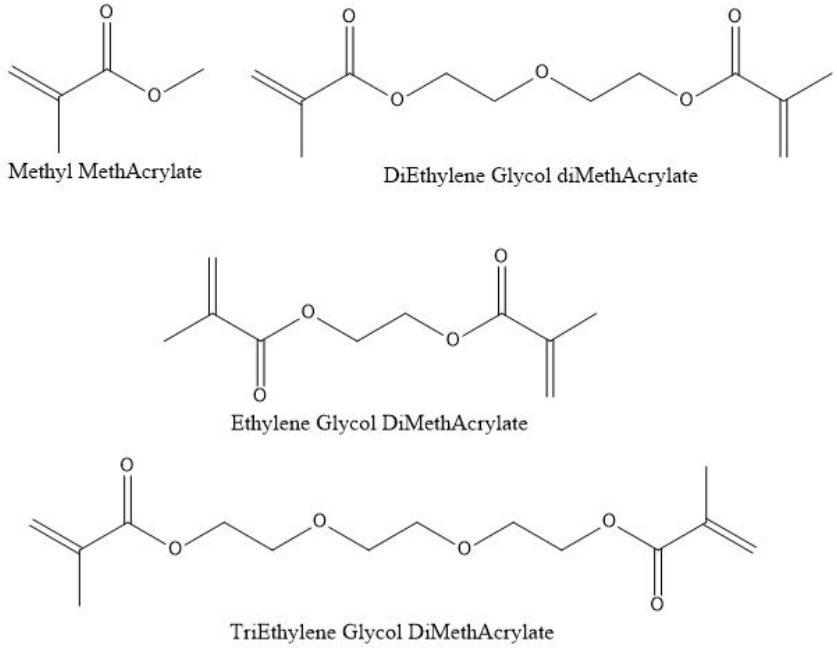

Figure I.11: Different types of viscosity controller monomer

Initiators

Monomer and diluent can only interact in the presence of catalyzed molecules. These molecules are influenced by light to edit a radicals to stimulate the reaction. It is called photo-initiators which exist in a ratio of 1 to 2 ٪of total size. There are two types of photo-initiators which combined two ways of polymerization: 1.type is chemo-polymerization: trimethylbenzoyl-diphenylphosphine oxide (TPO) , benzoyl peroxide (BPO) and 2.type is photo-polymerization: camphorquinone (CQ), phenanthrenequinone (PQ), benzophenone (BP) and 1-phenyl-1,2-propanodione (PPD) [13] . The photo-initiation system consists of photo-initiator and an electron donor or tertiary amine [16]. This system is stable in the presence of the oligomer at room temperature, as long as the composite is not exposed to light [12].

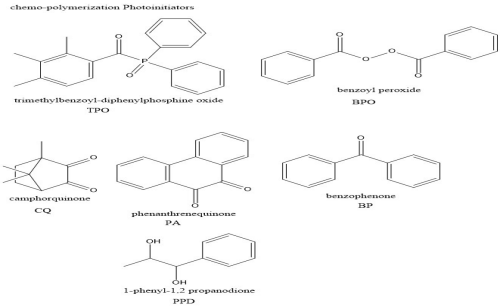

Figure I.12: Structure of photo-initiators

An example of the decomposition of benzoyl peroxide (BPO) is shown in **Figure I.13[17]**

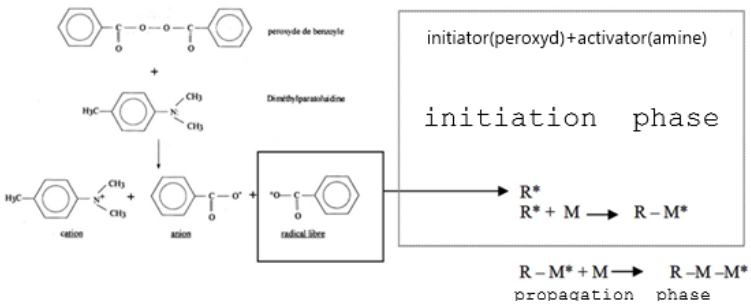

Figure I.13: Mechanism of decomposition of benzoyl peroxide in the presence of a tertiary amine

Inhibitors:

To avoid an untimely polymerization, it is necessary to take inhibitors. These inhibitors have a high affinity for free radicals. The purpose of inhibitors is to react with the free radicals that can form during their handling or their storage thus avoiding spontaneous polymerization. The hydroquinone monomethyl ether or BHT 2, 4, 6-tritertiary-butyl phenol are the major phenol-based inhibitors [14].

Filler particles (inorganic phase)

The inorganic phase consists of the charges that reinforce the material. These loads are linked to the matrix by means of a silane and allow in particular to increase the mechanical properties (tensile strength, bending, compression) of the composites. They also reduce the stresses due to shrinkage of polymerization, compensate for the too high coefficient of thermal expansion of the matrix phase and give the material its radio-opacity [17].

The most commonly used fillers can be [8]:

Minerals: these are alumina silicates, quartz, ceramics, borosilicate glasses and barium fluoride. Some heavy metal glasses can also be incorporated in order to obtain radiopacity, such as strontium, zirconium and barium.

Metals: tin, titanium and niobium are the most commonly used.

Organic: some composites can be fillers made up of already polymerized base resin. Others have their fillers already coated with base resin.

Coupling agents

Coupling agents are bi-functional molecules used to bind fillers to the resin [8] (**Figure I.14**).

There are currently a wide variety of coupling agents available on the market. (**Figure I.15[8]**).

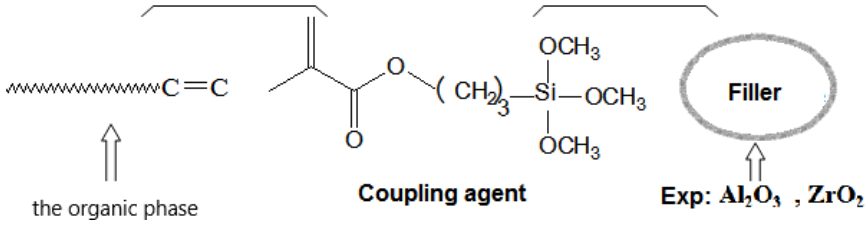

Figure I.14: Diagram interface matrix – load

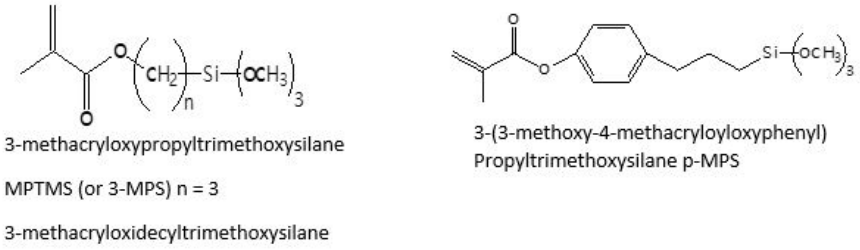

Figure I.15: Examples of light-curing methacrylate silanes.

Polymerization process of composite resin

There are 2 types of polymerizations:

Chemically activated composite resin (chemical polymerization)

Chemically activated composite resin consists of two tubes contain different paste each. Polymerization occurs when both pastes are mixed. The chemically activated composite resin reaction was shown in **Figure I.16[18]** . The tubes contain benzoyl peroxide initiator and aromatic tertiary amine activator (N, N-dimethyl-p-toluidine). When both pastes are mixed, benzoyl peroxide initiator and aromatic tertiary amine activator will produce a free radical and the polymerization starts [18].

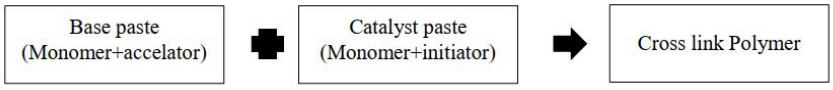

Figure I.16: Chemically activated composite resin (chemical polymerization)

Light activated composite resin (photopolymerization)

It is possible to cause a polymerization reaction by exposure to electromagnetic heaters such as UV light or visible light. There are the photons that serve as activators by acting on the "camphoroquinone" photo-initiators (absorption peak 466.5 nm) to make the composite[11]. The **figure I.17[18]** shows how the reaction is.

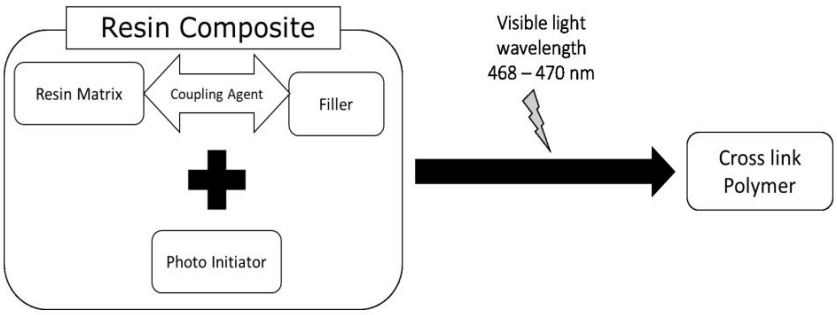

Figure I.17: Light activated composite resin (photopolymerization)

I.7 Classification of dental composites

Dental composites can be classified to macrofilled, microfilled, hybrid and nanofilled (**Figure I.18**[5])

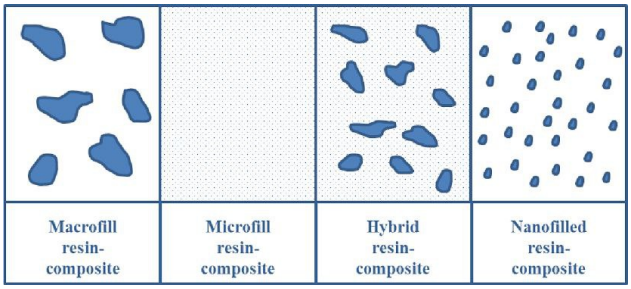

Figure I.18: Classification of dental composites on the basis of particle size and structure.

Macrofilled

Macrofilled composite resin or traditional composite resin has filler particles with $10-100\mu m$. It contains quartz filler, strontium or borium glass. The filler of macrofilled composite resin has relatively large size and hard, thus difficult to polish and may cause antagonist tooth to be eroded during contact [18].

Microfilled

Micro-fillers are particles smaller than 1 micron. It has a greater surface area in relationship to its volume than a large particle [23].

Hybrid

Hybrid composite resins contain a heterogeneous aggregate of filler particles. They are usually filled 70to 80%by weight with $0.04\mu mand1\mu mto5\mu m$ filler particles. The average particle size of hybrid composites is usually $\succ 1\mu m$. This mixture of fillers accounts for their excellent physical properties with high polishability when compared to the earlier macro-filled composites. Regrettably, one problem with hybrid composite resins is their inability to maintain their gloss[21].

Nanofilled

Nanofilled composites were recently introduced and they consist of nanomers (5 nm to 75 nm particles) and “nanocluster” agglomerates as the fillers. Nanoclusters are agglomerates (0.6 µm to 1.4 µm) of primary zirconia/silica nanoparticles (5 nm to 20 nm in size) fused together at points of contact, and the resulting porous structure is infiltrated with silane [21].

I.8 Properties of resin composite

Polymerization shrinkage

The polymerization shrinkage of methacrylate-based composites is among the most important causes of failure of composite restorations. The manufacturers claim that bulk-fill composites have a lower polymerization shrinkage than conventional composites. This study aimed to assess the polymerization shrinkage of five bulk-fill composites in comparison with a conventional composite[3].

Water absorption

The properties of composite resin fillings are affected by water absorption. Water behaves as a plasticizer and stress corrosion agent, weakening the particle matrix interface. Deterioration of the physical and mechanical properties can occur as a result of water ingress into dental resin composites in the oral cavity. This is primarily a result of the hydrolytic breakdown of the bond between silane and filler particles, the matrix/filler interface or the fillers [5].

I.9 Conclusion

Light-curing dental composites are widely used today; amalgams mercury-based cement and silicate cement posing a lot of problems. Multiple improvements have been made to these materials in recent years. Nevertheless, some problems remain: the volume contraction of the material during the polymerization remains too high, the mechanical resistance for the cervical teeth is still too weak, and the aesthetic aspect could be improved. The addition of nanofillers is a promising way to improve these problems. The influence of these nanofillers on the photopolymerization reaction and their compatibilization with the organic matrix are still little studied. The synthesis of new monomers is a promising way to reduce the rate of this contraction.

Bibliography

[1] Child and adult dentition. https://teachmeanatomy.info/head/other/child-adult-dentition/, 2020.

[2] The five stages of tooth decay. https://www.grandarcadedental.com.au/post/stages-of-tooth-decay, 2020.

[3] M. Abbasi, Z. Moradi, M. Mirzaei, M. J. Kharazifard, and S. Rezaei. Polymerization shrinkage of five bulk-fill composite resins in comparison with a conventional composite resin. *J. Dent. (Tehran)*, 15(6):365–374, Nov. 2018.

[4] R. B. Ali. Etude physico-chimique des composites dentaires. Master's thesis, 2018.

[5] A. Alrahlah. *Physical, Mechanical and Surface Properties of Dental Resin-composites*. The University of Manchester (United Kingdom), 2013.

[6] S. O. Alsharif, Z. Arifin, B. M. Ishak, and A. B. Arriffin. An overview on dental composite restorative "white filling". *Annals Inter J Eng*, 8:95–100, 2010.

[7] S. C. Bayne. Beginnings of the dental composite revolution. *The Journal of the American Dental Association*, 144(8):880–884, 2013.

[8] S. Bayou. *Etude physico-chimique de formulations dentaires chargées*. PhD thesis, University of Houari Boumediene Alger, 2013.

[9] P.-E. Chaumont. *La photopolymérisation des résines composites: données actuelles*. PhD thesis, Université de Lorraine, 2012.

[10] Y. Delaviz. *Synthesis of Antimicrobial Oligomers and Their Related Polymers Using a Combination of Antibiotics for Dental Restorations and Adhesive Materials*. PhD thesis, University of Toronto (Canada), 2018.

[11] D. K. Dr Arfa. Les resin composite, 2009.

[12] V. Greig. Craig's restorative dental materials. *British Dental Journal*, 213(2):90–90, 2012.

[13] A. Kowalska, J. Sokolowski, and K. Bociong. The photoinitiators used in resin based dental composite—a review and future perspectives. *Polymers*, 2021.

[14] G. Naury. Étude de l'étanchéité des composites de site 2 par obturation conventionnelle versus compothixo de kerr®.

[15] P. E. Petersen, R. Baez, S. Kwan, H. Ogawa, W. H. Organization, et al. Future use of materials for dental restoration: report of the meeting convened at who hq, geneva, switzerland 16th to 17th november 2009. 2010.

[16] B. Pratap, R. K. Gupta, B. Bhardwaj, and M. Nag. Resin based restorative dental materials: Characteristics and future perspectives. *Japanese Dental Science Review*, 55(1):126–138, 2019.

[17] A. Raskin. Les résines composites. *Société francophone de biomatériaux dentaires*, 2010, 2009.

[18] Y. R. Riva and S. F. Rahman. Dental composite resin: A review. In *AIP Conference Proceedings*, volume 2193, page 020011. AIP Publishing LLC, 2019.

[19] C. Sarosi, M. Moldovan, A. Soanca, A. Roman, T. Gherman, A. Trifoi, A. M. Chisnoiu, S. Cuc, M. Filip, G. F. Gheorghe, et al. Effects of monomer composition of urethane methacrylate based resins on the c= c degree of conversion, residual monomer content and mechanical properties. *Polymers*, 13(24):4415, 2021.

[20] G. Secci. Manuel d'hygiène bucco-dentaire destiné à la formation de prophylaxistes. *Secours Dentaire International. Secours Dentaire International*, 2010.

[21] L. G. Sensi, H. E. Strassler, W. Webley, and R. C. Margeas. Direct composite resins: Case report.

[22] M. Simkova, A. Tichy, M. Dusková, and P. Bradna. Dental composites - a low-dose source of bisphenol a? *Physiological research / Academia Scientiarum Bohemoslovaca*, 69:295–304, 10 2020.

[23] M. S. Spille. Dental composites:a comprehensive review. *The Academy of Dental Learning and OSHA Training, LLC, designates thisactivity for 4 continuing education credits (4 CEs).*, 2012.

[24] J. Vreven, A. Raskin, J. Sabbagh, G. Vermeersch, and G. Leloup. Résines composites. *Encyclopédie Médico Chirurgicale [en ligne]*, 2005.

CHAPTER II

HYDROXYAPATITE

II.1 Introduction

The name "apatite" was given a century ago to a group of minerals that are often confused with other minerals such as amethyste and olioine. etc. HAp is considered as the most important one in many fields, especially biology.

In 1771 , Scheel noticed that bones contain calcium phosphate, and in the 19th century X-ray diffraction studies showed that the component abundantly present in mineral tissues is HAp[4].

Studies began decades ago for the synthesis and analysis of HAp, where calcium phosphate has been widely used in the field of orthopedics and dentistry due to its ability to bind to living tissues [16].

II.2 Structure and chemical formula

HAp is a phosphatic compound with the chemical formula $Ca_{10}(OH)_2(PO_4)_6$[11]. It belongs to the apatite family with the general formula $Me_{10}(XO_4)(Y)_2$[9] where

- **Me:** Divalent Cation ($Sn^{2+}, Ba^{2+}, Ca^{2+}$....)
- XO_4**:** trivalent anion ($OV_4^{3-}, OsA_4^{3-}, OP_4^{3-}$....)
- **Y:** monovalent anion $(HO^-, Cl^-, F^-, Br^-$....)[1]

II.2.1 Crystal formula

Most of apatite crystallizes in the hexagonal system $(P6_3/m)$ [10]. So that the values of lattice coefficients a, b, c depend on the nature of ions Me, XO_4 and Y [17], where a =b= 9,418Åc=6.884Å, $\alpha = \beta = 90\gamma = 120^o$ [12]

The **figure II.1[14]** shows the crystal formula for Ca(2)HAp:

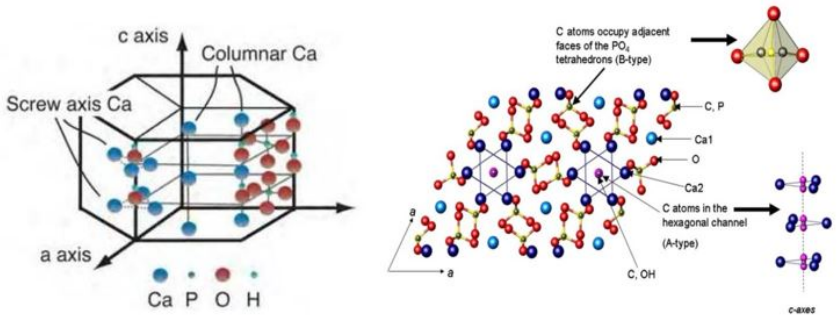

Figure II.1: (a) Atomic formula of HAp. (b) Representation along the (c) axis.

Figure II.1 shown that there are two tunnels, the first containing 4 Ca(1) ions placed at $C = 0$ and $1/2$, the Ca(1) cations surrounded by 09 atoms of oxygen forming a tunnel with a diameter approximately equal to $2.5A^o$, while the second tunnel has a diameter It ranges between (3 -5.4Å) , contains 06 other Ca(2) cations present in $C = 1/4$ $C = 3/4$ where they form two equilateral

triangles alternately around the helical axis. OH ions are located along this axis, coordinate ions Ca(2) equal to 7 [12]. To be more clear, the distribution of the atoms in the crystal is as follows:

Position of the ten calcium atoms:

Four atoms occupy the Ca(I) position, two of which are at position z=0 and the others at z=0.5. They thus form the columns parallel to c, respectively at x=1/3, y=2/3 and x=2/3, y=1/3.

The other six atoms occupy the Ca(II) position with three of them forming a triangle at z=1/4 and the others at z=3/4.

Positions of the hydroxides:

They are arranged in a column on the axis parallel to c at x=0, y=0 and z=1/4 and z=3/4.

Positions of phosphate ions:

They are found on a tetrahedron from level z=1/4 to level z=3/4. It is this pattern that gives apatite its stability.

The high chemical reactivity of apatites stems from the presence of colinear channels with the c axis. Indeed, it is possible to consider the partial or total replacement of the anion located in the tunnel by other anions such as chlorine, fluorine, etc. in order to obtain, for example, chloro- or fluoroapatites[8].

II.3 Preparation methods

Calcium phosphate attracts great interest due to its chemical structure close to the inorganic phase of the calcified tissue, and it forms a family of chemical compounds with different structures and forms such as HAp and is usually described by the Ca/P ratio of about 1.67 as in biological HAp.

Several techniques have been developed to synthesize HAp. These techniques are: [19]

II.3.1 Precipitation

The most widely studied and common method, also called chemical precipitation or wet precipitation, yields a large amount of HAp in the absence of organic solvents(the schema in **Figure II.2[21]**). This method depends on two types of reactions:

1. neutralization reaction (acid + base)
2. Reaction between two salts of HAp manufactured by chemical precipitation. pH, temperature, initial concentration of the reactants, speed of acid addition and shaking speed are the factors that control the degree of purity and crystallization of the resulting HAp [6].

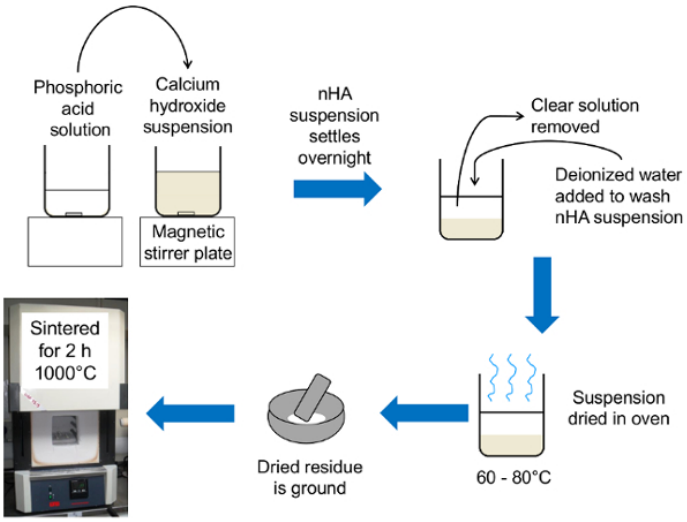

Figure II.2: Synthesis of precipitation.

II.3.2 Sol - gel method

This method depends on the polymerization of n(RO)M organic matter and then hydrolysis, monitoring the alkoxide in the solution, the condensation of the monomer to an oxo bridge and then the organic oxide. The gradual polymerization forms oligomers and then polymers, i.e., the viscosity increases(the schema in **Figure II.3[20]**).

These polymeric solvents play a role in gels that allow the material to be easily formed [7]

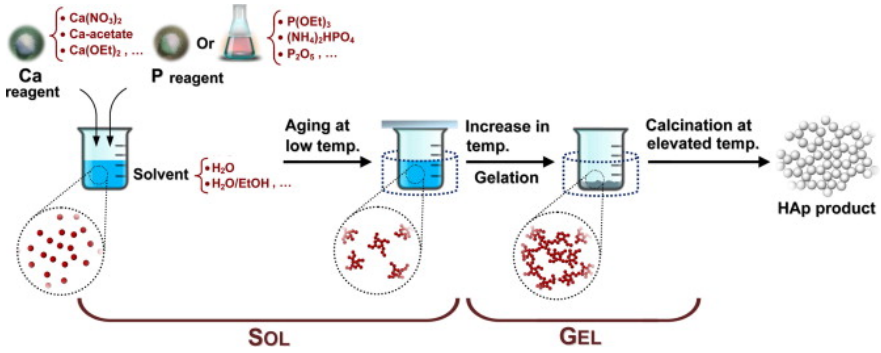

Figure II.3: The manufacture of hydroxyapatite by the sol-gel method.

II.3.3 Hydrothermal manufacturing

It is based on a technique consistiong of hydrothermal synthesis by heating a mixture of several reactions at a temperature of more than 100 °C and high pressure (at a temperature of <1) to increase the temperature in the evaporation of water(the schema in **Figure II.4[13]**).

A recent study by Maseru Yosimra where the latter synthesized HAp.[15]

$$10CaCO_3 + 6.H_3PO_4 \longrightarrow Ca_{10}(PO_4)_6(OH)_2 + 8H_2O + 10CO_2$$

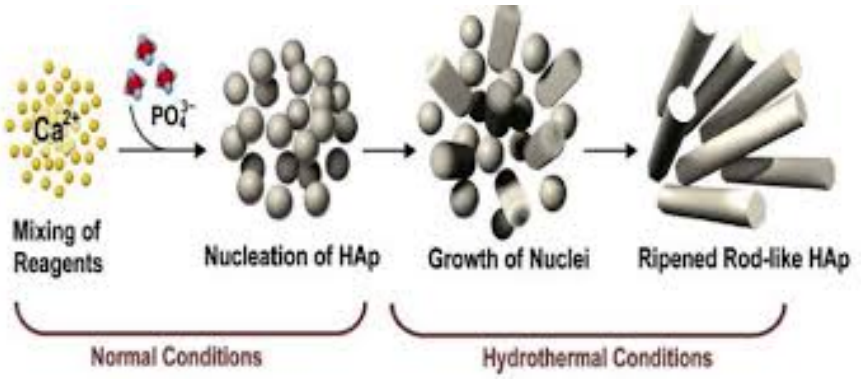

Figure II.4: Hydroxyapatite synthesis using hydrothermal method

II.3.4 Dry method

Hydroxyapatite is obtained in this way by heating a mixture of trimetallic phosphate $M_3(PO_4)_2$ with metal hydroxide $M(OH)_2$ at relatively high temperatures (1200 - 900) degrees Celsius and the following reaction illustrates this [18]:

$$6.M_3(PO_4)_2 + 2.M(OH)_2 \longrightarrow 2.M_{10}(PO_4)_6(OH)_2$$

The schema in **Figure II.5[20]**

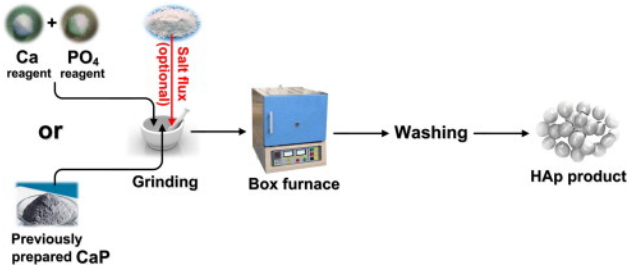

Figure II.5: Manufacture of hydroxyapatite by dry method

II.3.5 The liquid phase method

This technique relies on two processes: mixed decomposition and sedimentation. The first process is by adding the cation salt Me into a solution of the anion salt XO_4, then the precipitate is washed and dried. The disadvantages of this method are that it requires a lot of materials and is rather slow.

While the second process depends on the neutralization of milk lime by adding phosphoric acid, this reaction allows obtaining large amounts of HAp and faster than the first [7].

II.3.6 Manufacturing from industrial resources

HAp produced partially or entirely from biological sources is better accepted by living organs due to the physic-chemical similarity to human bone apatite, and biological sources are divided into groups such as extract from the shells of basil and biological waste.....

The most famous way to prepare HAp is the extraction of biological waste, specifically from cow bones, scales, fish bones ...Due to the interface and economical yield resulting from the recovery of this waste, this extraction requires heat treatment in order to eliminate all traces of organic matter from simple calcification [6].

The **figure II.6[2]** shows that.

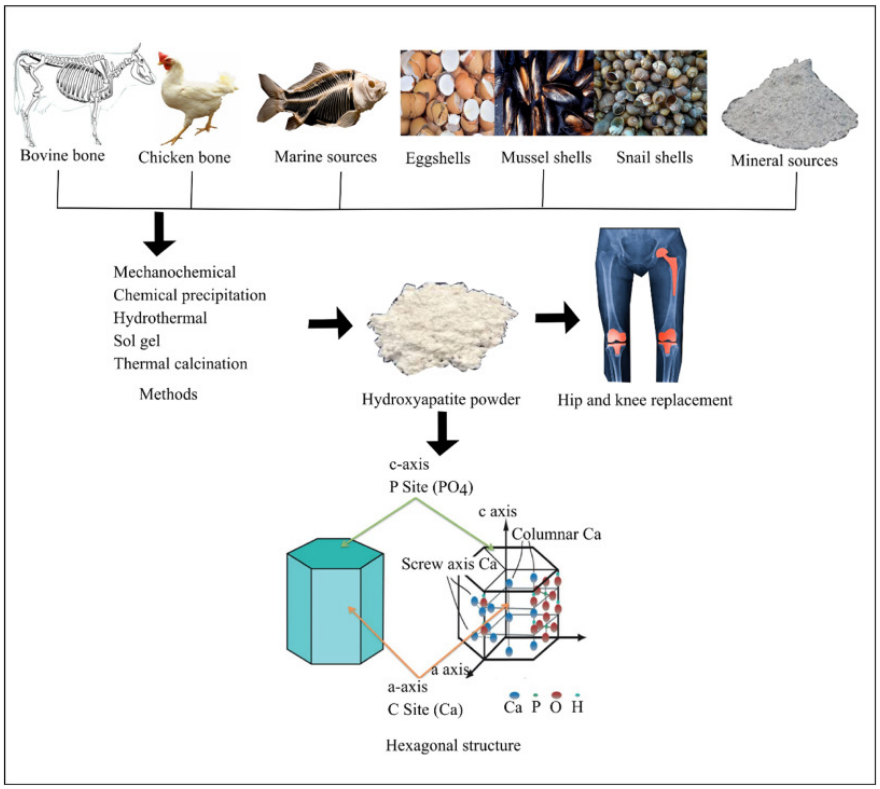

Figure II.6: Manufacture of hydroxyapatite from biological sources

II.3.7 Microwave method

It is a technique mainly used as the source of the article (calcium nitrate and ammonium phosphate) and when compared with the autoclave method, the manufacturing time and temperature of this garden house will spread in the house. [3]

II.4 Effect of different manufacturing methods on the properties of hydroxyapatite

The **Table II.1 [10]** shows many different sizes, shapes, and stoichiometric ratios that can be obtained for HAp and thus the multiplicity of factors that are likely to modify its main interaction.

Table II.1: Comparison of hydroxyapatite obtained by different methods.

Manufacturing method	Ca/P	Morphology	Microscope image Electron
Hydrothermal $Ca(NO_3)_2.H_2O$, $HPO_4(NH_4)_2$, $200^0C, 24h$	1.67	Obtaining particles having 100-600 nm elongated rods and 10-60 nm diameter	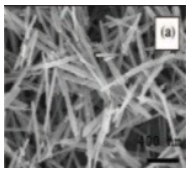
Hydrothermal $Ca(OH)_2$, $Ca(HPO_4)_2.H_2O$, $109^0C, 1-3h$	1.67	Hydroxyapatite appears as needles 130-170 nm long, 15-25 nm wide, SBEt: $31-43m^2/g$	
Hydrothermal $Ca(HPO_4)$, $Ca(CO_3), 140^0C$, 2h	/	preferential growth along the C-axis to yield hexagonal rods, 200 nanometers wide and a few microns long	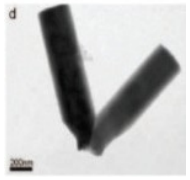
Hydrothermal $Ca(OH)_2$, $Ca(HPO_4)_2.H_2O$, $120^0C, 24h, pH = 9$	/	Elongated particles 600 nm long and 40 nm wide	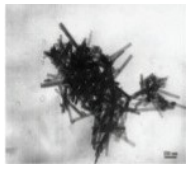
Hydrothermal $Ca(OH)_2$, $Ca(NO_3)_2, Na_2HPO_4$ $180^0C, 24h$, PVP (polyvinylpyrrolidone)	/	Elongated nanoparticles are 25-20 nanometers in diameter, a few hundred nanometers, and a few micrometers long.	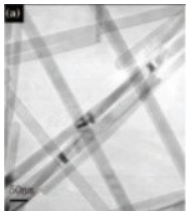

Hydrothermal $Ca(NO_3)_2$, $NaHPO_4$, $200^0C, 1h, pH = 11$	1.63	Elongated particles of medium size 6-18 μm	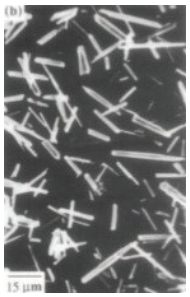
Sol-gel $Ca(NO_3)_2$, $H_3(HPO_4)$, $50^0C, 24h$ heat treatment	1.67	Spherical particles have a diameter of$100\mu m$	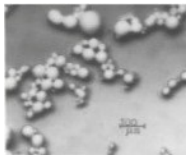
Sol-gel $Ca(NO_3)_2.H_2O$, $KH_2(HPO_4)$, $pH = 9, RT, 48h$	1.67	Hexagonal nanoparticles are stick-shaped, elongated 70-60 nm and 400-500 nm in diameter.	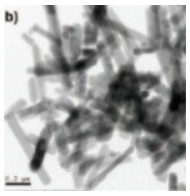
Sol-gel $Ca(NO_3)_2.H_2O$, $KH_2(HPO_4)$, $pH = 9, 37^0C, 3min$	1.64	Spherical particles with a diameter of 20-40 nm	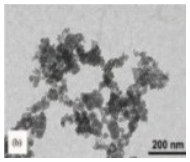
Sol-gel $(CH_3)_3P$, $Ca(NO_3)_2.H_2O$, $6days, RT, 16h, 60^0C$	1.67	Nanoparticles from 90-150 nm It forms a lumpy porous structure	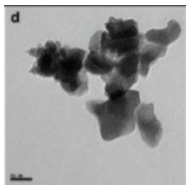

Dry TCP, $Ca(NO_3)_2.H_2O$, $2h, 1150^0C$or $8h, 1000^0C$	1.67	Agglomerated particles 18-20 micrometers in diameter	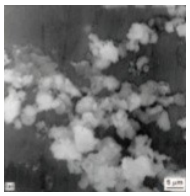
Microwave method $Ca(NO_3)_2.4H_2O$, $Na_2HPO_4, EDTA$ $19min, 600W$	1.67	Clumps have a different size between 50 nanometers and 4 micrometers Finally, crystals of 10-25 nm of mixed morphology are formed: Rods have a length of 15 nm and a diameter of 5 nm and an ellipse 16nm x 27nm	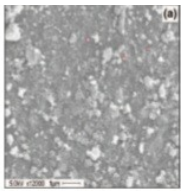
Microwave method $Ca(NO_3)_2.4H_2O$, $(NH_4)_2HPO_4, EDTA$ $45min, 800W$	/	We get fields of 20-50 nm while with EDTA We get rods 50-100 nm	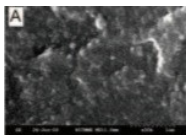
Precipitation $Ca(NO_3)_2.4H_2O$, $(NH_4)_2HPO_4, EDTA$ $(NH_2)_2CO$, $80^0C, 12h, pH = 8$	1.607	Elongated particles 200-300 nm long and 20 nm wide	
Precipitation $Ca(NO_3)_2.4H_2O$, $(NH_4)_2HPO_4, EDTA$ $80^0C, 24h, pH = 10.5$	1.67	Nodular particles with a relative diameter of 100-200 nm	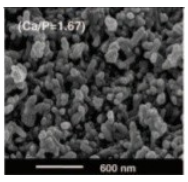

II.5 Hydroxyapatite Applications:

In the industrial field: Hydroxyapatite is used as a stationary phase in high-performance liquid chromatography to separate nucleic acids, proteins, and vitamins (vitamin D3). Hydroxyapatite is used as a catalyst in the polymer industry to remove water and hydrogen from primary alcohols [12] .

In the environmental field: Because of its iodine exchange capacity, hydroxyapatite has been used as a disinfectant for toxic elements (heavy metals) in polluted water [5] .

In the field of biomedicine: Because of its great similarity with biological apatite, hydroxyapatite is used in the form of granules or ceramic pieces to fill bone spaces. In otolaryngology, hydroxyapatite is used to achieve a bone-reconstructive prosthesis to replace the three bones of the ear (the malleus, the incus and the stirrup). [5].

The main advantage of HAp is the establishment of strong chemical bonds with bone due to its very close formation to calcified tissue [12].

II.6 Conclusion

It can be concluded that haydroxyapatite is synthesized in several different methods, such as: precipitation, hayd-rothermal, sol-gel, microwave, dry method, liquid phase method, and from industrial resources. Researchers in this field are involved in solving various challenges and difficulties related to the synthesis of HAp. However, research is continuing to discover other methods of synthesis of haydroxyapatite that are more economical.

Bibliography

[1] A. B. Z. A. T. T. A. A. BEGHOURA. Etude physico-chimique comparative entre l'hydroxyapatite élaboré à partir des précurseurs naturel et synthétique. 2014.

[2] P. Arokiasamy, M. M. Al Bakri Abdullah, S. Z. Abd Rahim, S. Luhar, V. A. Sandu, H. Noorina, and M. Nabiałek. Synthesis methods of hydroxyapatite from natural sources: A review. *Ceramics International*, 2022.

[3] I. Bahlali. *Extraction de l'hydroxyapatite a partir de l'os bovine*. PhD thesis.

[4] P. Balk. *Connaissances actuelles sur le revêtement hydroxyapatite des implants en titane*. PhD thesis, UHP-Université Henri Poincaré, 2005.

[5] Y. Belmamouni. Contribution à l'élaboration et à la caractérisation de biocéramiques nanocomposites à base d'hydroxyapatite substituée en silicium/nanotubes de carbone multiparois. 2014.

[6] S. Boussaria and H. Djebabri. Préparation et caractérisation des hydroxyapatite. Master's thesis, Université Mohamed Khider de Biskra, 2019.

[7] O. Britel. Modélisation et optimisation par la méthodologie des plans d'expériences de la synthèse: De l'hydroxyapatite phosphocalcique, du phosphate tricalcique apatitique, du phosphate de calcium apatitique carbonate. 2007.

[8] E. Chassot. *Mise en oeuvre de méthodes nucléaires et de diffraction pour l'analyse de la structure de l'hydroxyapatite dopée et des transferts d'éléments métalliques à partir de biomateriaux implantés in vivo*. PhD thesis, Université Blaise Pascal-Clermont-Ferrand II, 2001.

[9] N. Demonet. *Etude physico-chimique de depots plasma duplex alumine/hydroxyapatite pour applications medicales. Relations elaboration/structure/proprietes (dissolution, adherence, contraintes residuelles)*. PhD thesis, Paris, ENMP, 1998.

[10] S. Diallo-Garcia. *Hydroxyapatites, un système basique atypique modulable par la synthèse: vers l'identification des sites actifs*. PhD thesis, Paris 6, 2012.

[11] A. El Yacoubi. *PROPRIETES STRUCTURALES D'HYDROXYAPATITES SILICATEES ET ELABORATION DES SYSTEMES COMPOSITES A BASE D'ORTHOPHOSPHATE D'ARGENT/HYDROXYAPATITE EN VUE D'APPLICATIONS PHOTOCATALYTIQUES ET ANTIBACTERIENNES*. PhD thesis, Université Ibn Tofail, Faculté des sciences, Kénitra, Maroc, 2018.

[12] N. E. G. G. A. Z. Fayza. Adsorption du chrome par une hydroxyapatite à basede test d'oursin paracentrotus lividus(lamarck 1816). Master's thesis, Université Abdelhamid IbnBadis-Mostaganem, 2019-2020.

[13] D. F. Fitriyana, R. Ismail, Y. I. Santosa, S. Nugroho, A. J. Hakim, and M. S. Al Mulqi. Hydroxyapatite synthesis from clam shell using hydrothermal method: A review. In *2019 International Biomedical Instrumentation and Technology Conference (IBITeC)*, volume 1, pages 7–11. IEEE, 2019.

[14] M. Ishikawa. *Synthesis of Hydroxyapatite/Nanocellulose composites*‖. PhD thesis, Tese, 2014.

[15] D. Kherifi. *Synthèse de l'hydroxyapatite par voie sol-gel*. PhD thesis, Université Mohamed BOUDIAF de M'Sila, 2017.

[16] A. Lucas-Girot, F. Z. Mezahi, M. Mami, H. Oudadesse, A. Harabi, and M. Le Floch. Sol–gel synthesis of a new composition of bioactive glass in the quaternary system sio2–cao–na2o–p2o5: comparison with melting method. *Journal of Non-Crystalline Solids*, 357(18):3322–3327, 2011.

[17] D. Marchat. *Fixation du cadmium par une hydroxyapatite phosphocalcique: étude cinétique et thermodynamique*. PhD thesis, Limoges, 2005.

[18] A. Mechay. *Elaboration des biomatériaux apatitiques nanostructurés en milieux polyols: caractérisations physico-chimiques et études mécaniques après compaction par spark plasma sintering*. PhD thesis, Paris 13, 2014.

[19] V. P. Orlovskii, V. S. Komlev, and S. M. Barinov. Hydroxyapatite and hydroxyapatite-based ceramics. *Inorganic materials*, 38(10):973–984, 2002.

[20] M. Sadat-Shojai, M.-T. Khorasani, E. Dinpanah-Khoshdargi, and A. Jamshidi. Synthesis methods for nanosized hydroxyapatite with diverse structures. *Acta biomaterialia*, 9(8):7591–7621, 2013.

[21] C. J. Wilcock, P. Gentile, P. V. Hatton, and C. A. Miller. Rapid mix preparation of bioinspired nanoscale hydroxyapatite for biomedical applications. *JoVE (Journal of Visualized Experiments)*, (120):e55343, 2017.

CHAPTER III

PHOTO-POLYMERIZATION

III.1 Introduction

There are two forms to provide the activation energy required to induce chemical reactions, either in the form of light or in the form of radiation, where thermal chemical reactions have been used for a long time, and photochemical reactions have been used during the last half of the twentieth century[1]. Photo-polymerization is based on the use of light instead of heat, which is one of the most important scientific fields that allows us to provide many challenges and tremendous opportunities for researchers, scientists, and engineers in many disciplines and scientific applications, In the past few decades, many difficulties have been overcome in the field of photo-polymerization, and the worldwide market for UV-curable systems treatment of one billion dollars in 1995.

It is working on the production of new materials by converting monomers into polymers, and photo-polymerization is one of the best methods of expanding and fasting in the production of materials with an annual growth of more than 15 ٪in the next several years.
[5]

Photo-polymerization is also credited with improving several complex industries in different fields, especially in the fields of electronics, optical engineering, and medical fields. It has historically been credited with photography and printing materials and its application to electronic and mechanical devices, and it is the main reason for the development of lithography. Where optical images are formed by photo-polymerization, [7] and enter into the manufacture of dental bio-materials[1] .

III.2 Polymerization

III.2.1 Definition

Polymerization is a chemical reaction in which a large number of small molecules called monomers are linked together to form a large molecule with a high molecular weight called polymer [12]. Polymerization is carried out in several ways, but most of them are based on two principles: addition polymerization and condensation polymerization .

III.2.2 Polymerization in addition

It is a chemical chain reaction in which monomers are added together to form long chains called polymers without forming any secondary molecules. And they are in three types: the ring–opening reaction, radical polymerization, ionic polymerization .

III.2.2.1 The ring-opening reaction

It is a polymerization reaction in which the cyclic monomers are opened to form a linear polymer. Ethylene imine and epoxy resin reactions are the two most important reactions in dentistry for this type of polymerization.

III.2.2.2 Radical polymerization

This reaction includes radicals and consists of the cleavage of a carbon-carbon bond of one of the monomers by an activator. We often find this reaction in dentistry and it is divided into three steps:

- Initiation.
- Diffusion.
- Termination.

III.2.2.3 Ionic polymerization

This reaction can be initiated by a cation or an anion. It consists of three phases: initiation, diffusion and termination (the termination phase is what distinguishes this reaction from other polymerization reactions). [3]

III.2.3 Condensation polymerization

It is a polymerization reaction that takes place through steps and upon reaction a by-product is released, which is often water. [12]

III.3 Photo-polymerization

III.3.1 Definition

A photo-polymerization reaction is by description a chain reaction whose initiation step is photo-chemical in nature. The principle of the reaction of photo-polymerization consists of active species to initiate the polymerization. Once the reaction has started, the fluid monomer turns into a solid polymer. If the monomer is multi-functional (prossesing at least two reactive functions), we obtain a reticulated three-dimensional network [9, 11](**FigureIII.1[9]**).

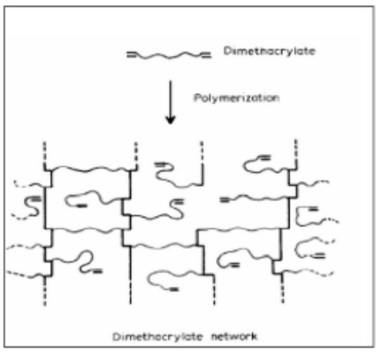

Figure III.1: Formation of three-dimensional network by photo-polymerization

III.3.2 Principle

Photo-polymerization is a polymerization process under ultraviolet light. In most cases, we need to use a small molecule called a photo-initiator. Without irradiation, these molecules are in the fundamental state. When enough energy photons are absorbed, the molecule becomes excited, causing electron transfer from the HOMO (highest occupied molecular orbital) to the LUMO (lowest unoccupied molecular orbital). These excitations result in the formation of radicals or ions, either by homolytic cleavage or withdrawal of hydrogen from the proton donor compound. In the presence of the monomer, these active species can initiate polymerization(**Figure III.2[13]**).

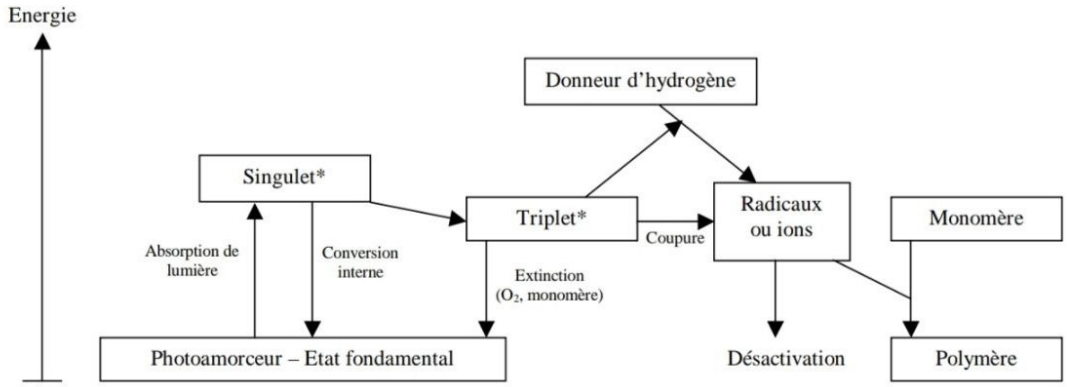

Figure III.2: Diagram of the photo-polymerization process

III.3.3 Photo-polymerization mechanism

One or more photo-initiators are added to the resin to initiate the reaction. The most commonly used photo-initiator in dentistry is a combination of camphorquinone and a tertiary amine. The reaction steps are the same as encountered in conventional polymerization processes: propagation, then termination. Thus, photo-polymerization is a free radical-forming or cationic polymerization reaction in which the initial reaction is initiated by a photonic activator. The photon is absorbed by the chromophore site of the molecule, which then produces a reactive species that causes the

monomer to be converted into a polymer. Compared to self-curing resins, light-curing composites offer many advantages, including higher percentage of filler (strength, durability), remarkable uniformity, very long working time, on-demand polymerization, and superior aesthetics[3].

III.3.4 Photo-polymerization reactions

There are two major classes of radical photo-polymerization and which are differentiated according to the type of photo-initiator used and the nature of the active center[2].

III.3.4.1 Cationic photo-polymerization

This reaction has the advantage of being insensitive to atmospheric oxygen. Furthermore, when the irradiation is terminated, the polymerization can continue without terminating reactions , in addition, this type of polymerization makes it possible to obtain better adhesion to the resin-coated carrier. Cationic photo-polymerization processes generally involve two classes of photo-initiators: those that produce Bronsted acids. Those that generate Lewis acids are especially capable of polymerizing vinyl ether-type monomers of heterocyclic monomers[13].The cationic photo-initiators used in cationic photo-polymerization are: onium salts and organometallic salts (**figure III.3[1]**).

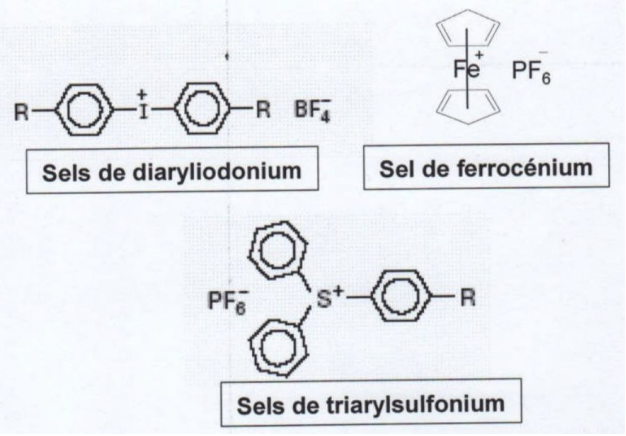

Figure III.3: Some examples of cationic photo-initiators

In the presence of hydrogen donor (RH), under the action of UV radiation, these photo-initiators are converted from Bronsted acid.

$$Ar_2I^+, BF_4^- + RH \xrightarrow{h\upsilon} ArI + Ar^\bullet + R^\bullet + HPF_4$$

$$Ar_3S + PF_6^- + RH \xrightarrow{h\upsilon} Ar_2S + Ar^\bullet + R^\bullet + HPF_6$$

The acid thus formed is capable of initiating the cationic polymerization of monomers of ether , lactone , epoxide, cyclic ether , epoxysilicone type . This sort of photo-initiator is especially utilized in dental formulations containing epoxy resins[1] .

Reaction mechanism [13] The mechanism is the same whatever the onium salt used taking into account the triarylsulfonium salt , the photopolymerization mechanism is as follows:

- Initiation:

$$Ar_3S^+ + X^- + RH \xrightarrow{h\upsilon} Ar_2S + Ar^\bullet + R^\bullet + HX$$

- Propagation:

$$HX + M \rightarrow HM^+ + X^- HM^+X^- + nM \rightarrow H - (M)_n - M^+X^-$$

- Termination

  By transfer to the monomer:

$$H - (M)_n - M^+X^- + M \rightarrow M_{n+1} + HM^+X^-$$

  By spontaneous transfer :

$$H - (M)_n - M^+X^- \rightarrow M_{n+1} + H^+X^-$$

  By transfer to a mobile hydrogen compound:

$$H - (M)_n - M^+X^- + HX \rightarrow H - M_{n+1} - M^+A^- + H^+X^-$$

III.3.4.2 Radical photo-polymerization

Free radical photo-polymerization is an addition polymerization reaction in which the initiation step is triggered by a photo-initiator. Addition polymerization is a chain reaction that forms a polymer from simple molecules (monomers). Radical polymerization consists of the cleavage of one carbon-carbon double bond in the monomer by an activator. This response consists of three steps: initiation, propagation and termination [3].

Radical photo-initiators : Species capable of initiating radical polymerization photo-chemically can be classified into two main families:

photo-initiators type 1:

This class of photo-initiators includes aromatic carbonyl compounds that undergo homolytic cleavage of a σ bond when exposed to UV radiation . two types of cut can take place:

- cut at carbonyl (Norrish type 1) :

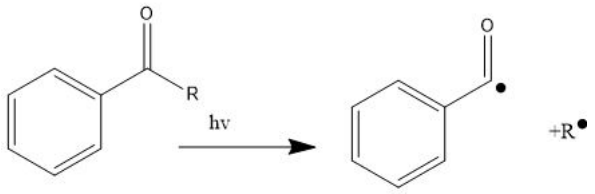

- cut in α of the carbonyl :

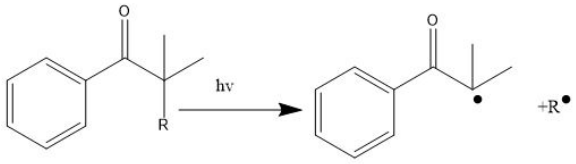

Some examples of radical photo-initiators are shown in **Figure III.4[1]**

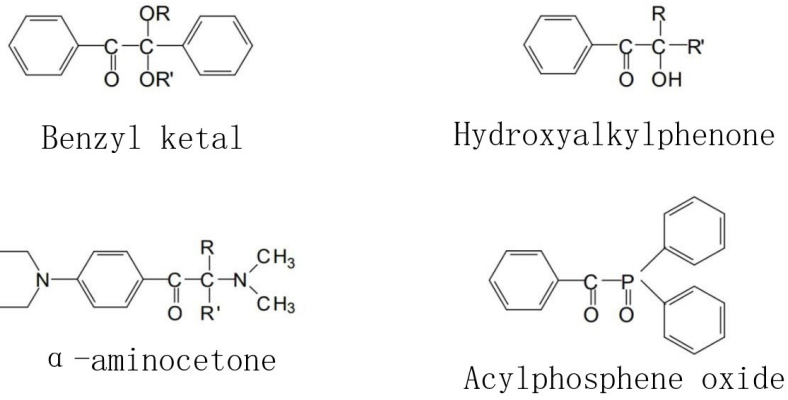

Figure III.4: Some examples of radical initiators type 1

Photo-initiators type 2 :

In the presence of UV radiation , these photo-initiators remove protons from unstable hydrogen-containing molecules and generate two radicals(**Figure III.5[13]**).

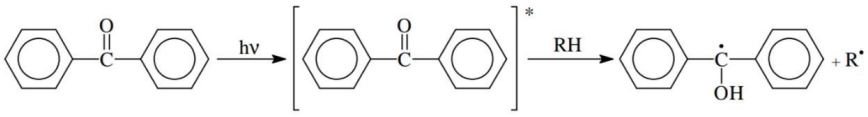

Figure III.5: Benzophenone activation principle

Two examples of type 2 photo-initiators are shown in **Figure III.6[1]**:

Reaction mechanism : In the most of cases , a radical polymerization reaction includes 4 steps : initiation, propagation , transfer and termination . without going into the small print of the kinetics , we will express , within the case of photosensitive systems , the speed of every step within the following way :

Figure III.6: Examples of type two radical photo-initiators

1. Initiation :

$$A \rightarrow A^* \rightarrow R^\bullet + R^\bullet$$

$$Va = 2\phi_a I_{abs} \; with \; I_{abs} = 2,3 I_0 \varepsilon \ell [A]$$

$$R^\bullet + M \rightarrow RM^\bullet$$

2. Propagation:

$$RM_n^\bullet + M \rightarrow K_{tr} RM_{n+1}^\bullet \quad V_p = K_p [RM_n^\bullet][M]$$

Transfer :

$$V_t r = K_{tr}[RM_n^\bullet][R] \quad RM_n^\bullet + R \rightarrow K_{tr} RM_n H + R^\bullet$$

3. Termination:
Monomolecular :

$$V_t = 2K_t[RM_n^\bullet] = V_a(EQS) \quad RM_n^\bullet + R^\bullet M_m^\bullet \xrightarrow{K_t} RM_n^\bullet M_m R^\bullet$$

Bimolecular :

$$V_t = 2K_t[RM_n^\bullet]^2 = V_a(EQS) \quad RM_n^\bullet + R^\bullet M_m^\bullet \xrightarrow{K_t} RM_n^\bullet M_m R^\bullet$$

In the case of monofunctional monomers, assuming the quasi-stationary (EQS) and a bimolecular termination, $V_t = 2K_t[RM_n^\bullet]^2 = V_a$ from where $[RM_n^\bullet] = \frac{V_a}{\sqrt{2K_t}}$. the rate of polymerization is then written:

$$V_p = \frac{K_p}{K_t^{0.5}} (2,3\phi\varepsilon I_0 \ell)^{0.5} [M][A]^{0.5}$$

With: K_p: Propagation rate constant.
K_t: Termination rate constant.
ϕ: Initiation quantum yield .
ε: Molar extinction coefficient.
I_0: Incident radiation intensity.
$[A]$: Photo-initiator concentration.
$[M]$: Monomer concentration[13].

III.3.5 Factors influencing the efficiency of polymerization

The factors influencing the efficiency of polymerization can be classified into two categories: intrinsic factors, dependent on the characteristics of the restorative material which are:

- The type and concentration and efficiency of the photo-initiator .
- Viscosity, monomers and fillers.
- Optical properties.

And extrinsic factors which are:

- lamps and emission spectra.
- Types of irradiation .
- Temperature.
- Positioning the lamp tip.
- Radiation exposure, power and irradiation time [6].

III.4 Light sources used in dentistry :

The light emitted by light sources that are used in dentistry is visible light (blue light). These sources are of two types:

1. Halogen lamps equipped with a filter avoiding infrared radiation and allowing irradiation between 400 and 500 nm.
2. Light –emitting diode (LED) lamps whose length of monochromatic emission wave is specifically centered on the absorption band of the photo-initiator(**Figure III.7[1]**).

Figure III.7: The different lamp used in dental offices.

III.5 Degree of conversion:

The degree of conversion is the percentage of double bonds C=C in monomers that convert to single bonds C-C during the polymerization reaction. The conversion is never complete (100٪), for dental resins often ranging from 50 to 60٪[8]. The conversion rate depends on factors such as:

- Irradiation time .
- The size and charge rate.
- The power of the light source of the lamp.
- The nature of organic matrix.

The transmittance increases as the fillers approach the refractive index of the matrix. Hence, the photon source itself will polymerize a greater thickness of the material [4, 10].

III.6 Conclusion

In this chapter, we presented a bibographical reminder on polymerization and its most important reactions, then we went directly to photo-polymerization, which is one of the most important polymerization reactions that take place in the presence of a light source. Photo-polymerization has played an important role in the field of dentistry in recent years due to the widespread use of light-treated dental compounds today, where traditional fillings have been known to cause many problems to replace them with resin, which is a safer biological material that is formed mainly from the reaction of photopolymerization.

Bibliography

[1] S. Bayou. *Etude physico-chimique de formulations dentaires chargées*. PhD thesis, University of Houari Boumediene Alger, 2013.

[2] M. Bolla, A. St-Georges, and D. Fortin. Photopolymérisation des composites dentaires: quoi de neuf? *Journal dentaire du Québec*, 39:149–156, 2002.

[3] P.-E. Chaumont. *La photopolymérisation des résines composites: données actuelles*. PhD thesis, Université de Lorraine, 2012.

[4] J.-L. Halary and F. Lauprêtre. *De la macromolécule au matériau polymère. La théorie néo-darwinienne de l'évolution: La théorie néodarwinienne de l'évolution*. Humensis, 2015.

[5] M. Kaur and A. Srivastava. Photopolymerization: A review. *Journal of Macromolecular Science, Part C: Polymer Reviews*, 42(4):481–512, 2002.

[6] L. Métais. Adhésion et photopolymérisation: données actuelles et évaluation des pratiques dans un échantillon de praticiens du finistère. *UFR d'odontologie de Brest*, 2013.

[7] K. Nakamura. *Photopolymers: photoresist materials, processes, and applications*. CRC Press, 2018.

[8] A. Raskin. Les résines composites. *Société francophone de biomatériaux dentaires*, 2010, 2009.

[9] M. Soh and A. U. Yap. Influence of curing modes on crosslink density in polymer structures. *Journal of dentistry*, 32(4):321–326, 2004.

[10] F. Stahl, S. H. Ashworth, K. D. Jandt, and R. W. Mills. Light-emitting diode (led) polymerisation of dental composites: flexural properties and polymerisation potential. *Biomaterials*, 21(13):1379–1385, 2000.

[11] G. Vanherle. Posterior composite resin dental restorative materials. *P Szulic*, pages 109–137, 1985.

[12] P. Weiss. La chimie des polymères. *Société Francophone de Biomatériaux Dentaires umvf. univnantes. fr/odontologie/enseignement*, pages 2009–2010, 2010.

[13] O. Zovi. *Fonctionnalisation et photopolymérisation de l'huile de lin en vue de l'élaboration de nouveaux matériaux sans émissions de composés organiques volatiles (COV)*. PhD thesis, INSA de Rouen, 2009.

CHAPTER IV

Synthesis and characterization of hydroxyapatite (HAp)

IV.1 Introduction

In this chapter, HAp ($Ca_{10}(PO_4)_6(OH)_2$) has been prepared by two methods. The first method was precipitation which used chicken eggshells. The second one was the hydrothermal method which used a teflon autoclave. To check the prepared compounds, bovine bone has been brought as a natural source.

IV.2 The products' use

In this work, we used 2 methods to prepare the inorganic phase(precipitation and hydrothermal) which is HAp. For the precipitation method, chicken eggshells (white and brown) were used as a source of calcium (figure IV.1) . The chemical products were used in the hydrothermal method. As mentioned before, hydroxyapatite is found in natural sources: bovine bones, fish bones, and others, to confirm the compounds synthesized in the two methods, bovine bones (femur) were compared with standard product (**Table IV.1**).

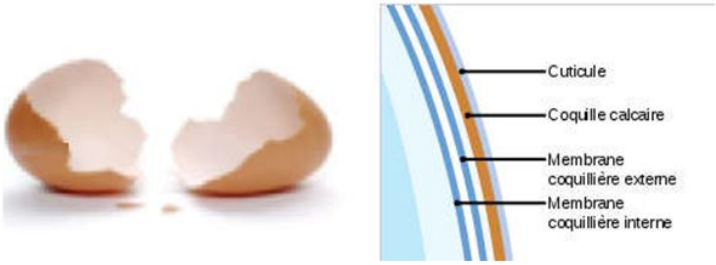

Figure IV.1: Chicken brown eggshell anatomy

Table IV.1: Reagents and solvents used in this synthesis

Reagents	Solvents
H_3PO_4 (86٪), $CaCl_2$ (100 ٪), chicken eggshells (white and brown)	NH_4OH, NH_4Cl, H_2O

IV.3 Synthesis of hydroxyapatite

IV.3.1 Preparation of HAp from natural source:

Bovine bone N-HAp (femur) was washed and boiled in water for 30min to remove the lipid membrane and tissue was employed, after that the bone was dried, ground and sieved with a sieve of 50 µm (this powder is symbolized by by N-HAp).

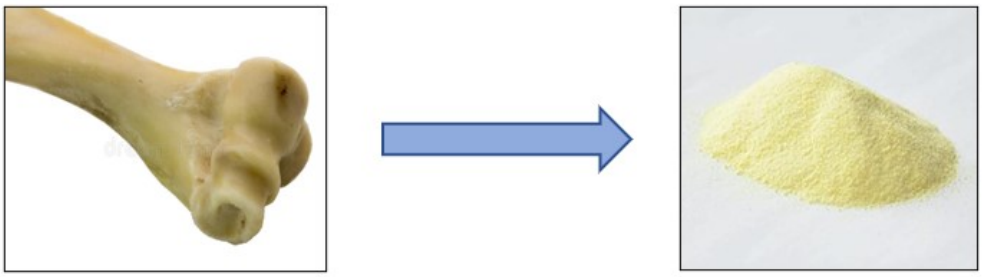

Figure IV.2: Preparation of HAp from natural source

IV.3.2 Synthesis of HAp by precipitation:

Preparation of the eggshell powder Chicken eggshells were collected, washed with tap water and then soaked for a day, after that the membrane was separated from the shell, which was leaved in the sun to dry, grounded and sieved with a sieve of 50 ($\approx 50\mu m$). The powder was further calcined in at 900°C in a tubular oven for one hour. The expected reaction is as follows:

$$CaCO_3 \longrightarrow CaO + CO_2 \nearrow$$

HAp particles were synthesized by precipitation method from solution A and B.

Solution A: 0.925g of calcined eggshell (CaO) was taken from a beaker and dispersed in 25ml of distilled water and stirred for 10 min to ensure complete dissolution of the powder. In this step, the CaO is transformed into$Ca(OH)_2$ according to the following reaction:

$$CaO + 2H_2O \longrightarrow Ca(OH)_2 + OH_2 + heat$$

Solution B: 0.720g of phosphoric acid H_3PO_4 is dissolved in 25ml of distilled water and stirred for 10 min. The aqueous solution B is added drop by drop ($\approx 150\mu l/s$) to the solution A. After the total addition of the phosphoric acid (solution B), the pH of the mixture is maintained above 10. The formation of a precipitate was observed at this point. The mixture is then stirred for 2 h and then maintained for 48 h at ambient temperature for its maturation. The expected reaction for this process is as follows:

$$10.Ca(OH)_2 + 6.H_3PO_4 \longrightarrow Ca_{10}(PO_4)_6(OH)_2 + 18.H_2O$$

The precipitate is separated from the mother water by filtration on Buchner and washed with distilled water and inserted into the centrifuge. It is then dried at 90°C for 24 hours to remove the absorbed water. The product is then ground into an agate mortar to obtain a very fine powder (this powder is symbolized by p-HAp(25°C)).

A quantity of the powder was calcined at 900°C for 2 hours in the oven (this powder is symbolized by p-HAp(900°C)).

NOTE: In this work white and brown eggshells were used as source of calcium. So the HAp obtained from white eggshells is symbolized by by p-HAp-w-(25°C) and p-HAp-w-(900°C) , and the powder form brown is symbolized by by p-HAp-b-(25°C) and p-HAp-b-(900°C).

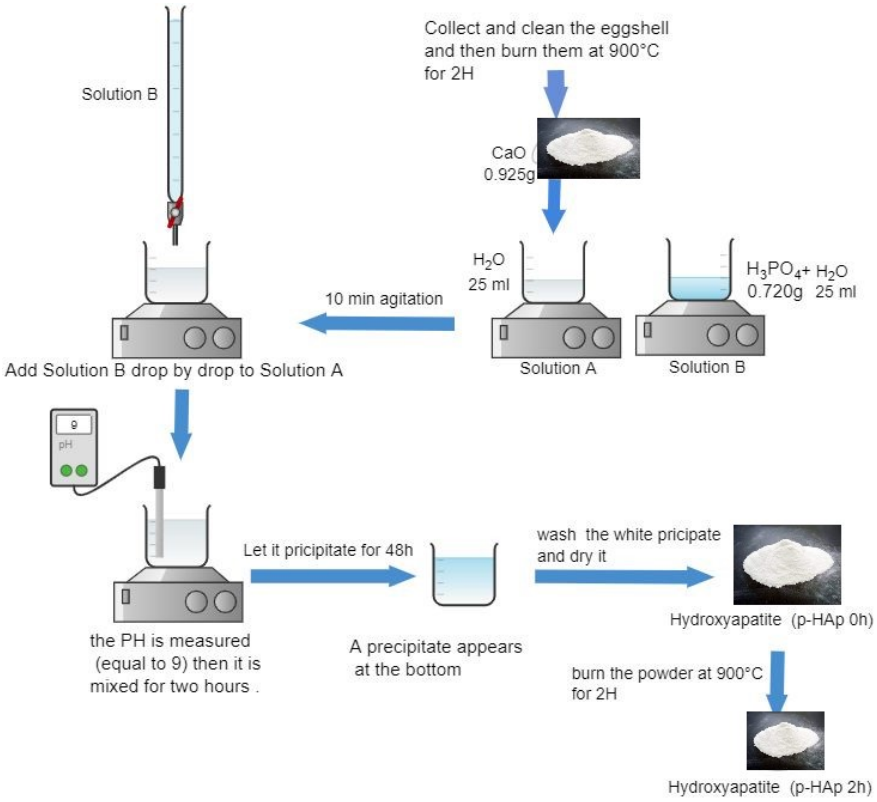

Figure IV.3: Protocol for precipitation method

IV.4 HAp synthesis by hydro-thermal method

A solution of phosphoric acid ($0.3mol/l\ H_3PO_4$) was added to a$0.5mol/l\ CaCl_2$ solution under continuous agitation for 2h at room temperature. A white precipitate was obtained by adding a 30℅solution of NH_4OH until reaching pH 9. The white precipitate was washed with distilled water and filtered under vacuum (this powder is symbolized by T-HAp 0h). The powder was then dispersed in a $0.1mol/lNH_4Cl$; the weight ratio between the precipitate and the solution was 1:10. The suspensions were placed in a stainless steel coated Teflon autoclave to receive hydro-thermal treatment at 150°C for 5h (T-HAp 5h). Finally, The resulting material is washed with distilled water and inserted into the centrifuge, dried and stored in the desiccator(look at annex). The product is then grounded into an agate mortar to obtain a very fine powder. The synthesis followed the equation:

$$10.CaCl_2 + 6.H_3PO_4 + 2.NH_4OH \longrightarrow Ca_{10}(PO_4)_6(OH)_2 + 18.HCl + 2.NH_4Cl$$

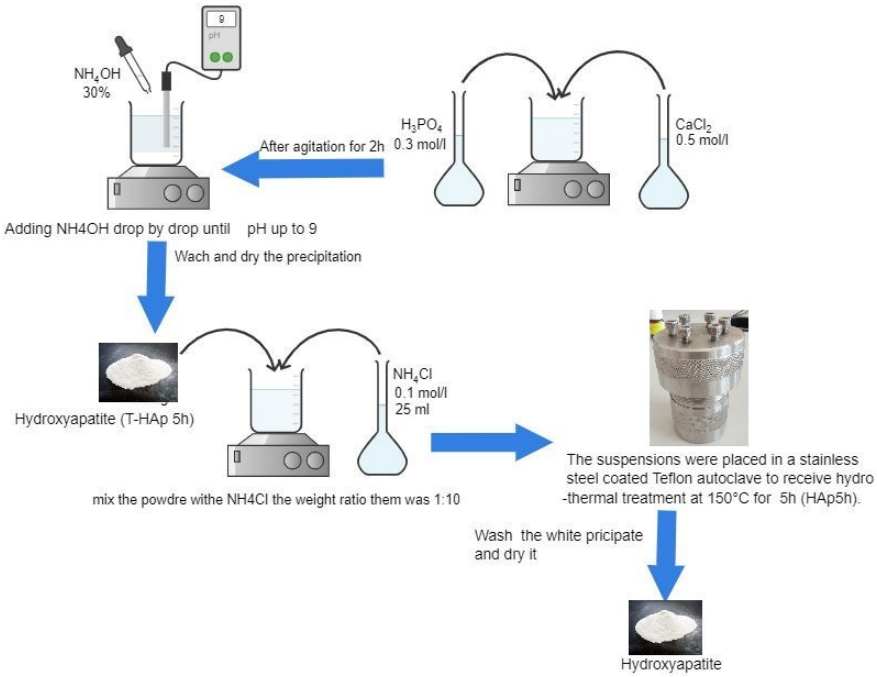

Figure IV.4: Scheme for hydro-thermal method

IV.5 Characterization of hydroxyapatite

IV.5.1 Fourier Transform Infrared (FTIR) analyses

The structure of synthesized HAp was characterized by a Fourier Transform Infrared device in ATR mode (FTIR-ATR). A quantity of the HAp to be analyzed is deposited in powder form on the ATR plate of the IR device.

IV.5.1.1 Characterization of natural hydroxyapatite (N-HAp):

The infrared spectrum of N-HAp bovine bone is shown in **Figure IV.5**:

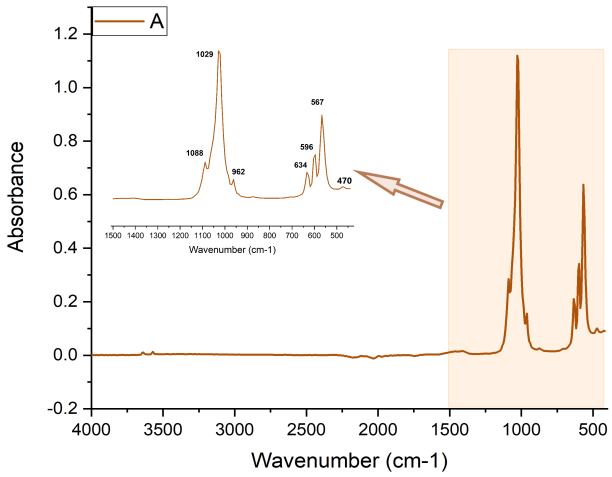

Figure IV.5: FT-IR spectra for N-HAp

The FTIR technique was used to study the composition of the HAp powder. Figure IV.5 shows the infrared spectra of HAp (N-HAp). In these spectra, peak placed at 634 cm^{-1} corresponds to the hydroxyl (OH^-) vibration groups. Furthermore, peaks at 470, 559, 596, 962, 1021 and 1088 cm^{-1} belonging to phosphate groups (PO_4^{3-}) were found. These functional groups are characteristic of stoichiometric (Ca/P=1,67) hydroxyapatite. Moreover, **Table IV.2** presents the list of functional groups, wave number, and type of vibration mode.

Table IV.2: FT-IR spectra characteristic peak of HAp from natural source

Wave number (cm^{-1})	Functional group	Vibration mode
470	PO_4^{3-}	-
567, 596	PO_4^{3-}	Bending
634	OH^-	Bending
962, 1029, 1088	PO_4^{3-}	Stretching

IV.5.1.2 Characterization of hydroxyapatite synthesized by precipitation(p-HAp)

The infrared spectra of samples p-HAp-w-(25°C) and p-HAp-w-(900°C) synthesized from white eggshells are show in the **Figure IV.6**:

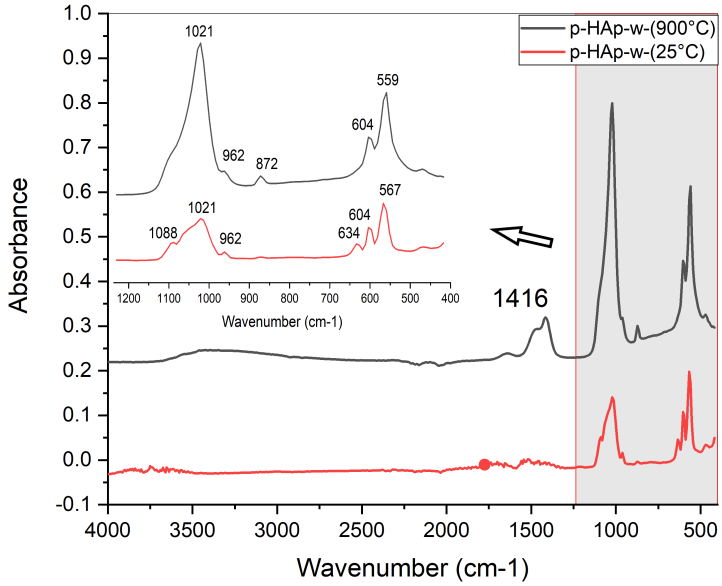

Figure IV.6: FT-IR spectra for p-HAp-w-(25°C) and p-HAp-w-(900°C).

The infrared spectrum of p-HAp-w(25°C) shows the presence of bands placed at 634 and 3570 cm^{-1} which correspond to the hydroxyl (OH^-) vibration groups. Furthermore, bands at 470, 567, 604, 962, 1021, and 1088 cm^{-1} belonging to phosphate groups (PO_4^{3-}) were found.

It should be noted that the heat treatment at 900 °C confused the areas between 1400-1600 cm^{-1} and 3500–4000 cm^{-1}, and the peak in 643 cm^{-1} disappeared after heating. Indeed, the IR spectrum of p-HAp-w (900°C) shows the presence of the elongation vibration band at 1416 cm^{-1} of the CO_3^{2-} ions resulting from the starting product $CaCO_3$. We also note a broad band around

3650 cm^{-1} and 3450 cm^{-1}, which indicates the H_2O absorbed in the sample and the OH^- of the HAp (at 3570 cm^{-1}). The peaks have been identified and illustrated in **Table IV.3**.

Table IV.3: FT-IR spectra characteristic peak of p-HAp-w-(25°C) and p-HAp-w-(900°C).

Wave number (cm^{-1})	Functional group	Vibration mode
470	PO_4^{3-}	-
559-567, 604	PO_4^{3-}	Bending
634	OH^-	Bending
872	HPO_4^{2-}	Stretching
962, 1021, 1088	PO_4^{3-}	Stretching
3750	OH^-	Stretching

The IR spectra of p-HAp-b-(25°C) and p-HAp-b-(900°C) samples synthesized by precipitation from brown eggshells are shown in **Figure IV.7**:

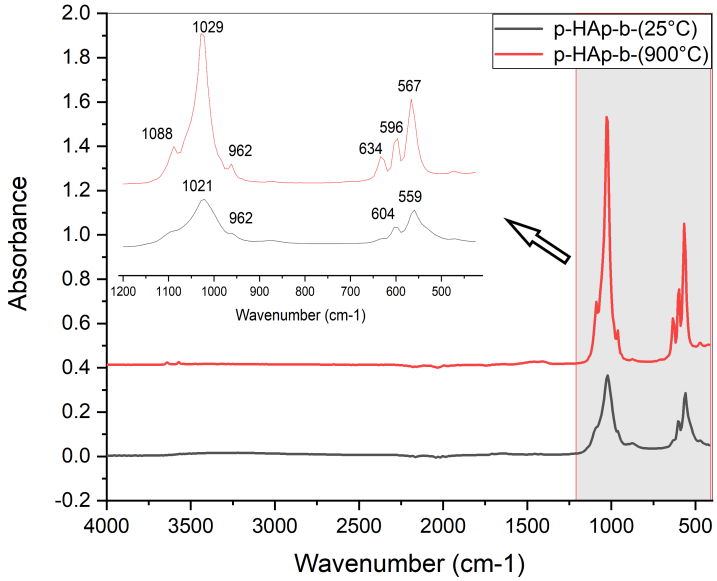

Figure IV.7: FT-IR spectra for p-HAp-b-(25°C) and p-HAp-b-(900°C)

Figure IV.7 shows the infrared spectra of p-HAp-b-(25°C) and p-HAp-b-(900°C). Bands at 470, 559-567, 596-604 and 1021-1029 cm^{-1} belonging to phosphate groups (PO_4^{3-}) were found. The peak at 872 cm^{-1} is referred to HPO_4^{3-} which did not react. The band placed at 634 cm^{-1} corresponds to the hydroxyl (OH^-) vibration groups.There are peaks that appear only after burning. The peaks have been identified and illustrated in the **Table IV.4**. We can also notice that the spectrum of p-HAp-b-(900°C) is almost identical to that of N-HAp bovine bone.

Table IV.4: FT-IR spectra characteristic peak of p-HAp-b-(25°C) and p-HAp-b-(900°C).

Wave number (cm^{-1})	Functional group	Vibration mode
470	PO_4^{3-}	-
559-567, 596-604	PO_4^{3-}	Bending
634	OH^-	Bending
962, 1021-1029, 1088	PO_4^{3-}	Stretching

IV.5.1.3 Characterization of hydroxyapatite synthesized by the hydrothermal (T-HAp)

FT-IR spectra for T-HAp 0h and T-HAp 5h is shown in the **Figure IV.8**

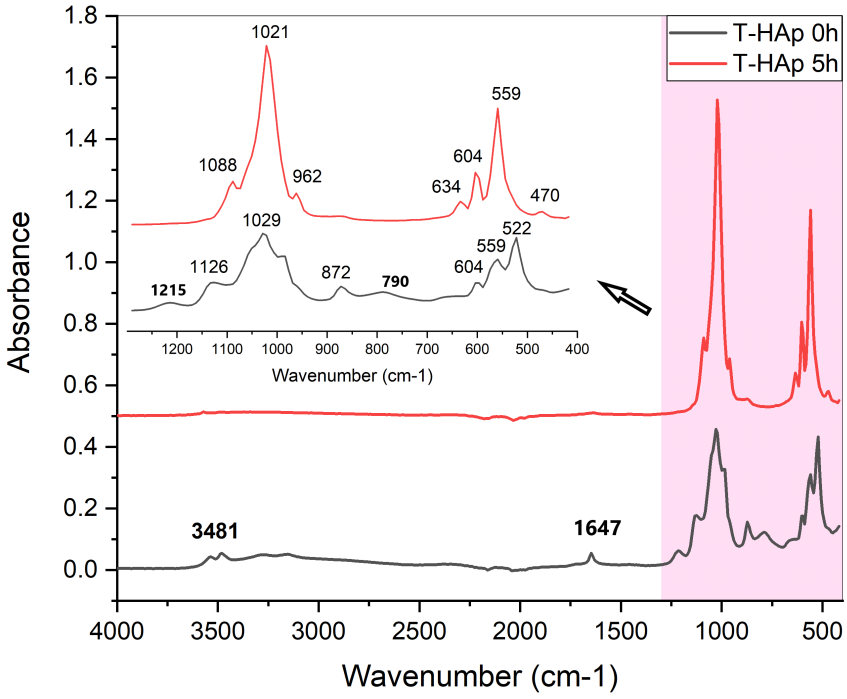

Figure IV.8: FT-IR spectra for T-HAp 0h and T-HAp 5h.

Figure IV.8 shows the infrared spectra of T-HAp 0h and T-HAp 5h. In these spectra, bands placed at 634, 3481 cm^{-1} correspond to the hydroxyl (OH^-) vibration groups. Furthermore, bands at 522, 559, 604, 962 and 1021-1039 cm^{-1} belonging to phosphate groups (PO_4^{3-}) were found. The peak at 873 cm^{-1} is refer to HPO_4^{2-} group which means that there is some molecules did not react. In this case, we see that the T-HPA(0h) spectrum became very clear after 5h of burning because there were some peaks that do not belong to HAp like 790 cm^{-1} which refers to DCPD (dicalcium phosphate dihydrate) and 1126 cm^{-1} refering to TCP (tricalcium phosphate), 1215 cm^{-1} refering to OCP (octa-calcium phosphate), and 1647 cm^{-1} which also refers to DCPA (anhydrous dicalcium phosphate). Consequently, the heat treatment at 150°C for 5 hours by autoclave makes the synthesis of the sample better. These functional groups are characteristic of stoichiometric hydroxyapatite. Moreover, **Table IV.5** presents the list of functional groups, wave number, and type of vibration mode.

Table IV.5: FT-IR spectra characteristic peaks of T-HAp 0h and T-HAp 5h.

heating time (h)	Wave number (cm^{-1})	Functional group	Vibration mode
0h	559, 604, 1029	PO_4^{3-}	-
	790	$Ca(HPO_4).2.H_2O$ (DCPD)	-
	873	HPO_4^{3-}	Bending
	634	OH^-	Bending
	1126	$\alpha and \beta - Ca_3(PO_4)_2$ (TCP)	-
	1215	$Ca_3(PO_4)_2.2,5.H_2O$ (OCP)	-
	790	$Ca(HPO_4)$ (DCPA)	-
	3470-2700	H_2O (DCPA)	-
5h	559, 604,634, 962	PO_4^{3-}	Bending
	1021-1029, 1088	PO_4^{3-}	Stretching
	3571	OH^-	Stretching

IV.5.1.4 Comparison of the best resulting samples

For a more precise analysis, the spectra of the final synthesized products were compared with the standard bands of hydroxyapatite. The comparison of the standard spectrum, N-HAp, p-HAp-w-(900°C), p-HAp-b-(900°C), and T-HAp 5h is shown in **Table IV.6**.

From the results in table IV.5, we notice that the values of the bands of the synthesized products almost resemble the standard values.

Table IV.6: Comparison of the best resulting samples

Simple	IR absorption bonds (cm^{-1})					
	OH^-	CO_3^{2-}	PO_4^{3-}	HPO_4^{2-}	OH^-	PO_4^{3-}
Standard	3570	-	1090, 1040, 960	-	634	603, 565
N-HAp	3645	-	1088, 1029, 962	-	634	596, 567, 470
p-HAp-w-(900°C)	3750	1409	1021	872	-	604, 559, 470
p-HAp-b-(900°C)	3645	-	1088, 1029, 962	-	634	596, 567, 470
T-HAp 5h	3571	-	1096, 1036, 962	-	634	604, 559, 470

IV.5.2 X-ray diffraction analyses

The results of X-ray diffraction (XRD) were compared (look at annex). It was noted that the results after burning were better, so it was processed. **Figure IV.9** represents samples p-HAp-w-(900°C), p-HAp-b-(900°C) and T-HAp 5h. The spectrum of p-HAp-w-(900°C), p-HAp-b-(900°C) is in good agreement with the reference model of pure hydroxyapatite (JCPDS no. 09-0432), and no characteristic peaks of impurities (**Figure IV.10**), such as calcium hydroxide and calcium phosphate, were observed, which means that the samples of phase-pure HAP. The thermal method is not similar to the reference which indicates that the crystal is not complete. The precipitate yielded broad and overlapping reflections, indicating its low crystallinity. The determined crystallite size (determined by the Scherrer equation), and crystal system from XRD of three samples of calcined HAp are given in **Table IV.7**.

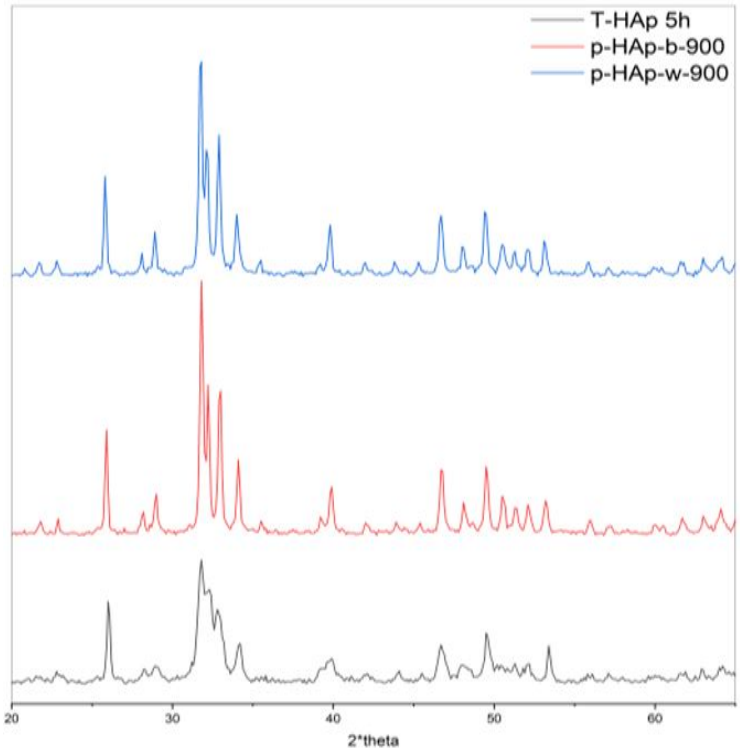

Figure IV.9: XRD patterns of p-HAp-w-(900°C), p-HAp-b-(900°C) and T-HAp 5h powders.

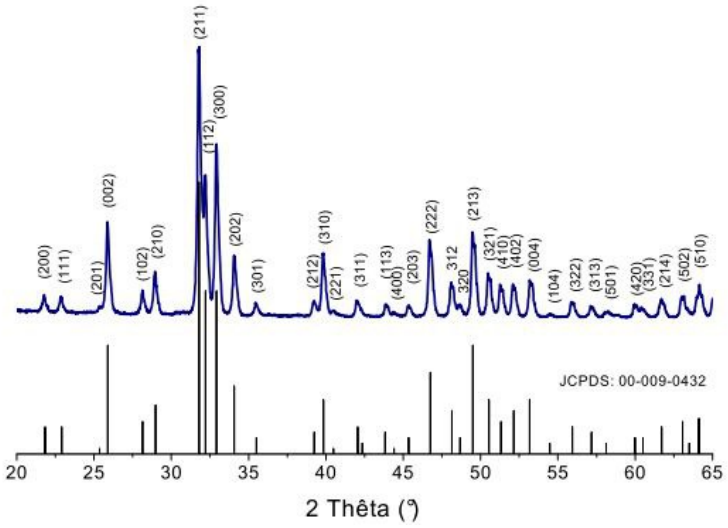

Figure IV.10: XRD pattern of pure hydroxyapatite .

Table IV.7: Crystallite size and parameters of the retinal structure of p-HAp-w-(900°C), p-HAp-b-(900°C) and T-HAp 5h

sample	standard	P-HAp-w-900°C	P-HAp-b-900°C	T-HA-p-5h
a,b- axis (A°)	9.42	9.44	9.44	9.42
c-axis (A°)	6.884	6.88	6.88	6.89
Crystallite size (nm)	-	0.349	0.234	0.259

IV.6 Conclusion

In this chapter, we synthesized hydroxyapatite with 2 different methods: the first was the precipitation method (we used white and brown eggshells as calcium source), and the second was

the hydrothermal method (which uses a teflon autoclave for thermal treatment). After FTIR and XRD analyses, we conclude that the heat treatment, whether by burning or autoclaving, contributes to the purification of the resulting compound and makes it more crystalline, as the compounds produced after heat treatment are purer and closer to the studied natural compounds.

Bibliography

1. P. A. F. Sossa,B. S. Giraldo, B. C. G. Garcia, E. R.Parra, and P. J. A.Arango, Comparative study between natural and synthetic Hydroxyapatite: structural, morphological and bioactivity properties. Matéria (Rio de Janeiro), 23, 2018.

2. J. K.Odusote, Y.Danyuo, A. D.Baruwa, and A. A.Azeez, Synthesis and characterization of hydroxyapatite from bovine bone for production of dental implants. Journal of Applied Biomaterials and Functional Materials, 17(2), 2280800019836829, 2019.

3. K. P.Malla,S. Regmi, A. Nepal, S. Bhattarai, R. J. Yadav,S. Sakurai, and R. Adhikari, Extraction and characterization of novel natural hydroxyapatite bioceramic by thermal decomposition of waste ostrich bone. International journal of biomaterials, 2020.

4. P. Shi, M. Liu, F. Fan, C. Yu, W. Lu, and M. Du, Characterization of natural hydroxyapatite originated from fish bone and its biocompatibility with osteoblasts. Materials Science and Engineering: C, 90, 706-712, 2018.

5. S. R.D. Krishna, A. Siddharthan, S. K. Seshadri, , and T. S. Sampath Kumar, . A novel route for synthesis of nanocrystalline hydroxyapatite from eggshell waste. Journal of Materials Science: Materials in Medicine, 18(9), 1735-1743, 2007.

CHAPTER V

Photopolymerization of dental composites filled with hydroxyapatite

V.1 Introduction

In this chapter, we will prepare two dental composites, using two types of filler. The first one with precipitated HAp and the second one with hydrothermal HAp. The organic phase was prepared by using TMPTMA as monomer, DEGDMA as diluent and as the initiation system for initiating the photo-polymerization reaction of four resins, which is a compound of camphorquinone (CQ) / N,N-dimethylaminoethyl methacrylate (DMAEMA).

This chapter will be more precisely devoted to the kinetic study of the reaction of photo-polymerization of these engineered resins. We will thus study the influence of the chemical composition chemical of the formulation and determine the kinetic parameters of the reaction of optimal dental resin photo-polymerization.

V.2 The products' use

For the organic phase, TMPTMA was used as monomer, DEGDMA as diluent and CQ/DMAEMA as initiator system. This solution was prepared in quantity for preparing 2g of organic phase. The **Figure V.1** shows the structure of the used material :

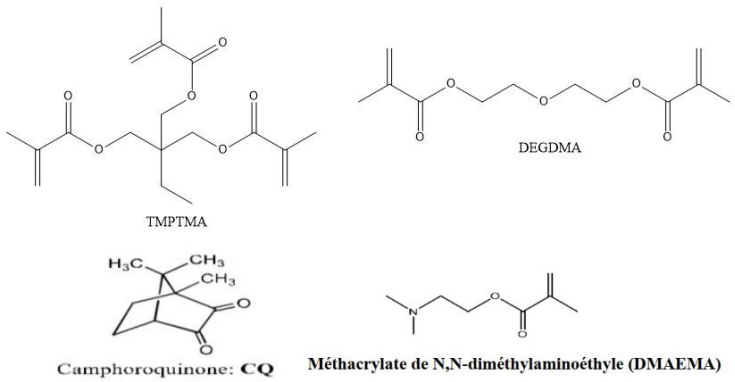

Figure V.1: Chemical structure of monomers and organic phase initiation system (resin).

The quantities of the used reagents are presented in table V.1 .

Table V.1: Quantities and physical properties of resins used in the composite.(M=molar mass, $\mu = viscosity$)

The components	Ratio (٪)	Quantity (g)	Physical properties
TMPTMA	48	0.96	M= 338 g/mol $\mu = 1.06g/mL$
DEGDMA	48	0.96	M= 214.22 g/mol $\mu = 1.087g/ml$
CQ	2	0.04	M= 166.220 g/mol
DMAEMA	2	0.04	M= 157.21 g/mol $\mu = 0.945g/mL$

For the inorganic phase, the compounds prepared in the third chapter4 were used (p-HAp-w-(900°C), ,and T-HAp 5h)

V.3 Preparation of experimental composites

The composite resins synthesized in our laboratory were prepared in two steps:

1. In the preparation of the reactive mixture (photopolymerizable resin), the mixture of TMPTMA and DEGDMA monomers with the CQ/DMAEMA priming system was carried out with magnetic stirring for 60 min at 25°C in the dark. The formulations obtained are stored in the cold and protected from light before their use to avoid any crosslinking reaction.

2. The hydroxyapatite filler dispersion in the photopolymerizable resin aids in the dispersion of the hydroxyapatite crystals. This dispersion was made by hand in sample boxes using a spatula.

V.4 Method for monitoring the light-curing reaction

V.4.1 Analytical technique

In order to follow the photo-polymerization kinetics of the prepared composite material, we used IRTF Fourier Transform Infra-Red spectroscopy in ATR mode. This technique is a powerful tool when trying to determine the conversion of a light-cured resin.

V.4.2 Preparation of samples analyzed by IR

The sample being studied, in liquid or pasty form, is placed directly on the ATR crystal (**FigureV.2**).The acquisition of the spectrum before and after photopolymerization is then carried out and recorded. During our study, the polymerization lamp used to polymerize the samples is a blue light type LED lamp (used in dental offices).

The analysis was carried out in a wave number range between 400 and 4000 cm^{-1}. The study range that interests us is between 1800 and 1550 cm^{-1}, **FigureV.3**, corresponding to the elongation vibration peaks of the C=C double bonds of the methacrylates at 1632 cm^{-1} and of the C=O groups at 1714 cm^{-1}.

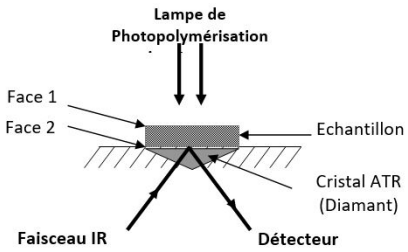

Figure V.2: Schematic representation of a sample positioned in contact with the crystal of the ATR-FTIR device.

V.4.3 Calculation of degree of conversion

The degree of conversion (DC) can be defined as the extent to which monomers react to form polymers or as the proportion of C=C double bonds that are converted to C-C single bonds. In the polymerization of bifunctional methacrylates, complete conversion is never achievable because diffusion restrictions in later stages of the polymerization reaction prevent a number of monomer molecules from reaching the reaction sites.

The determination of the degree of conversion of the polymerization reaction was carried out by using an FTIR Fourier transform infrared spectroscopy apparatus in ATR mode. The analysis was carried out in a wavenumber range between 400 to 4000 cm^{-1}, **Figure V.3** is corresponding to the elongation vibration peaks of the methacrylate double bonds at 1632 cm^{-1} and C=O groups at $1714cm^{-1}$.

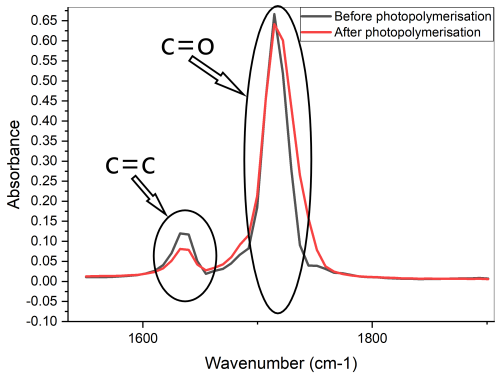

Figure V.3: FT-IR spectrum for C=C and C=O group before and after photo-polymerization.

The degree of conversion is the percentage of [C=C] double bonds that convert to [C-C] when of the polymerization reaction. Conversion to methacrylic double bonds can be calculated by measuring the absorbance to before and after the photo-polymerization reaction and using the following formula:

$$\text{DC}(\%) = \frac{\left(\frac{A_0^{1632}}{A_0^{1714}}\right) - \left(\frac{A_t^{1632}}{A_t^{1714}}\right)}{\left(\frac{A_0^{1632}}{A_0^{1714}}\right)} \times 100$$

Where:

- **DC:** the degree of conversion of methacrylic double bonds.
- A_0 : the initial absorbance of the methacrylate groups before photo-polymerization.
- A_t : the absorbance at time t of the methacrylate groups after photo-polymerization. The degree of conversion calculation was based on the height of the absorption bands of the IR peaks characteristics concerned.

V.4.4 Polymerization speed

The rate of the polymerization reaction (Vp) is the derivative of the conversion with respect to time:

$$Vp_t = \frac{d(DC_t)}{dt}(ins^{-1})$$

V.5 Effect of time on the degree of conversion:

In order to determine the time required for the reaction crosslinking of the organic phase, we exposed the samples to the light of the lamp at time intervals of 0 seconds to 80s. The calculation of DC at each instant is illustrated in **Table V.2**. The evolution curves of DC and Vp as a function of time for the TMPTMA/DEGDMA resin are represented in **Figures V.4 and V.5**.

Table V.2: The values of DC at each instant t

Time (s)	0	5	10	20	30	50	60	80
Peak height before polymerization C=C (cm)	0.11	0.10	0.09	0.075	0.067	0.064	0.064	0.063
Peak height before polymerization C=O (cm)	0.66	0.66	0.66	0.65	0.63	0.62	0.62	0.62
DC (٪)	0	7.93	19.65	29.46	35.26	37.74	37.71	37.73

The following curve represents the changes in the degree of conversion as a function of time:

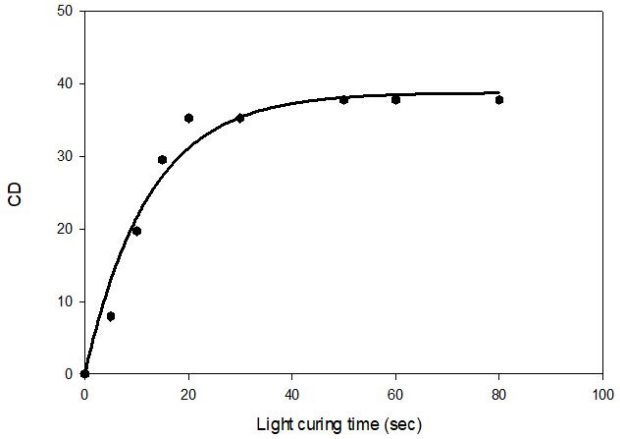

Figure V.4: The evolution of the DC of the methacrylate of resin (TMPTMA/DEGDMA) group as a function of the polymerization time

From the curve, we notice that the DC increases over the range from 0 to 50 seconds, indicating that the polymerization is not completed, but it proves after a time of 50 seconds and from it the time required for photo-polymerization is 50 seconds by DC equal to 37.73٪.

it should be noted that the optimum final conversion of the polymerization reaction remains less than 100%due to the transition to the glassy state which causes the blocking of the reactive species and stops the polymerization.

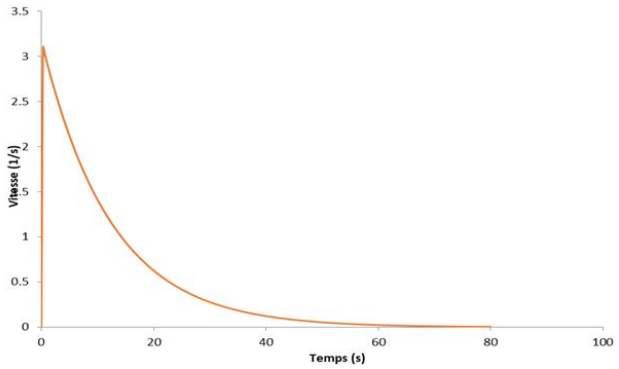

Figure V.5: Evolution of the polymerization rate as a function of resin time (TMPTMA/DEGDMA).

It is interesting to note that the photo-polymerization reaction of these formulations stops at 38%conversion rates (**Figure V.4**), indicating that the reaction medium still contain unresponsive methacrylate functions. This little explained by the gelification of the medium which decreases the mobility of the radicals and the polymerizable sites, and therefore the probability of encounter of the radical species and the double bindings methacrylates becomes very low. This stage is characterized by the gradual decrease in the rate of polymerization of formulations after the medium gelification. We arrive at the vitrification which causes the total blockage of reactive species that are trapped in the polymer network (**Figure V.5**). This translates into a gradual cessation of reaction.

V.6 Effect of filler ratio on the degree of conversion

The photo-polymerization of formulations containing HAp-w-(900°C) and T-HAp-(5h) hydroxapatites at different mass proportions ranging from 0 to 50%was studied. **Table V.3** groups together the DC values of the different formulations. The variations of the conversion according to the rate of loading for the various formulations are represented in **Figures V.6 and V.7**.

Table V.3: DC variation of composite different contents of hydroxyapatite from 0 to 50٪.

Filler type	Filler ratio (٪)	0	20	30	40	50
p-HAp-w-(900°C)	Peak height before polymerization C=C (cm)	0.11	0.11	0.11	0.11	0.10
	Peak height before polymerization C=O (cm)	0.66	0.65	0.65	0.65	0.52
	Peak height after polymerization C=C (cm)	0.06	0.07	0.07	0.07	0.03
	Peak height after polymerization C=O (cm)	0.62	0.63	0.62	0.61	0.016
	DC (٪)	37.72	33.70	33.43	33.20	17.25
T-HAp 5h	Peak height before polymerization C=C (cm)	0.11	0.11	0.11	0.11	0.10
	Peak height before polymerization C=O (cm)	0.66	0.63	0.61	0.59	0.23
	Peak height after polymerization C=C (cm)	0.06	0.07	0.06	0.07	0.04
	Peak height after polymerization C=O (cm)	0.62	0.076	0.61	0.59	0.23
	DC (٪)	37.72	27.77	31.76	24.72	6.41

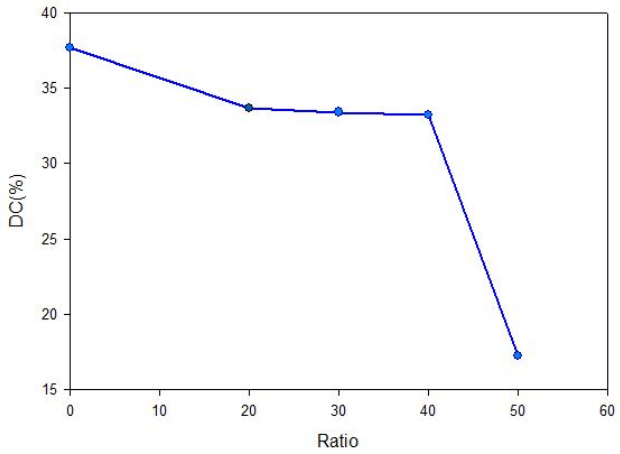

Figure V.6: DC variation of composite different contents of hydroxyapatite (p-HAp-w-(900°C).) from 0 to 50٪.

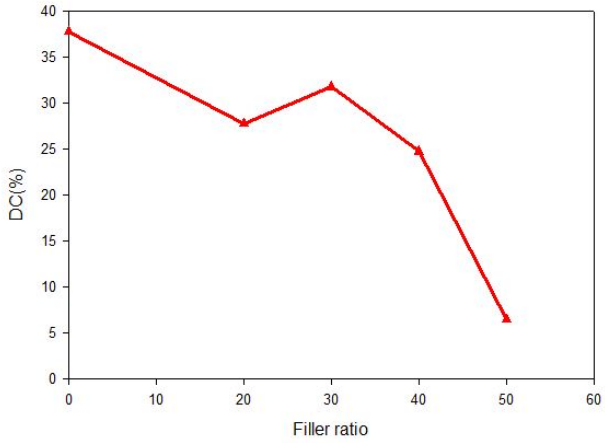

Figure V.7: DC variation of the composite at different hydroxyapatite (T-HAp 5h)contents from 0 to 50%.

The curves in the **Figures V.6 and V.7** show the changes in the degree of polymerization in terms of the filler ratio. We note in **Figure V.6** that there is no difference in the proportions for each of 20, 30 and 40%where the values of DC is 33%, but at 50 it decreases until 6.41%. The **Figure and V.7** shows that the DC not regular, since the better result is in 30%with DC 31.76. In the general case, it is observed for both systems, that the final conversion decreases when the filler content increases.

V.7 Effect of the filler type on the degree of conversion

A comparison having been made between the two composites comprising the hydroxyapatites P-HAp-w- (900° C.) and T-HAp 5h is represented in **Figure V.8**.

According to **Figure V.8**, it is noted that the composite comprises the charge of the hydroxyapatite P-HAp-w-(900° C.) gives better DCs compared to the composite T-HAp-(5h).

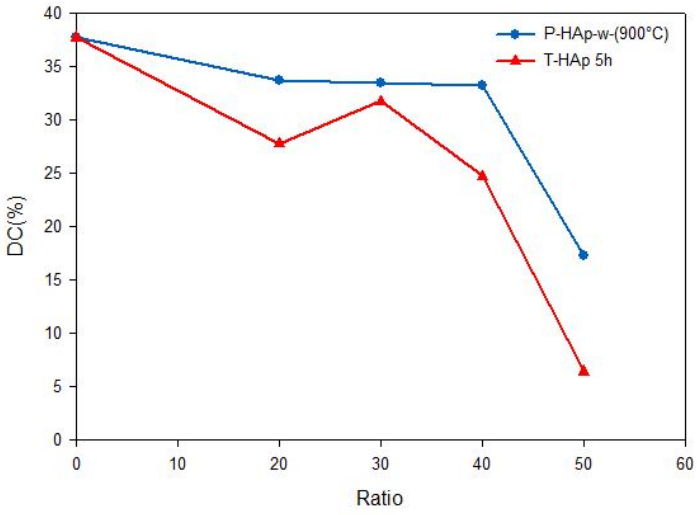

Figure V.8: Comparison of the two types of composites P-HAp-w-(900°C) and T-HAp 5h.

V.8 Conclusion

The study by FTIR/ATR spectroscopy allowed the determination of the degree of conversion (DC) of the elaborated composites. This study allowed us to conclude that:

- Methacrylate monomers polymerize very quickly under the action of visible light.
- The photo-polymerization reaction of the TMPTMA/DEGDMA resin is incomplete and remains less than 100%.
- The arrest of chain growth during crosslinking photo-polymerization is mainly due to the occlusion of polymer radicals in the three-dimensional matrix being formed.
- The incorporation of hydroxyapatite filler decreases the degree of conversion.
- The degree of conversion is conditioned by the content and the nature of the filler.

GENERAL CONCLUSION

In this work, new dental restorative materials photo-polymerizable under visible radiation were prepared. These materials have been reinforced with hydroxyapatite fillers.

In the first part, we synthesized hydroxyapatite based on various natural (chicken egg shells) and synthetic (with chemicals) sources. In order to compare and confirm the structure of the prepared hydroxyapatite, the samples were analyzed by infrared spectroscopy (IR) and by X-ray diffraction (XRD). The results obtained by IR and XRD after the heat treatment of the samples, made it possible to confirm the structure of the hydroxapatite$Ca_{10}(PO_4)_6(OH)_2$.

The second part of this work was devoted to the study of the polymerization reaction under visible radiation of a dental formulation based on TMPTMA (48%)/DEGDMA (48%) methacrylate resins, in the presence of a photo-initiator system. CQ (2%)/ DMAEMA (2%) and loads of HAps.

The effect of reaction time on the degree of conversion (DC) was studied by FTIR in order to determine the time required for the solidification of this formulation (uncharged). The measurements of the DC as a function of time made it possible to optimize the duration of the reaction which is 50 seconds with a degree of final conversion equal to 37.73. Finally, it should be noted that the optimum final conversion of the polymerization reaction remains less than 100%due to the transition to the glassy state which causes the blocking of the reactive species and stops the polymerization.

The influence of the HAp charge prepared by the two methods on the kinetics of the polymerization reaction of the charged formulations was also studied. The results obtained by FITR on the degree of polymerization show that the incorporation of HAp at different percentages infects the polymerization reaction.

ANNEX

Figure 1:Solution A

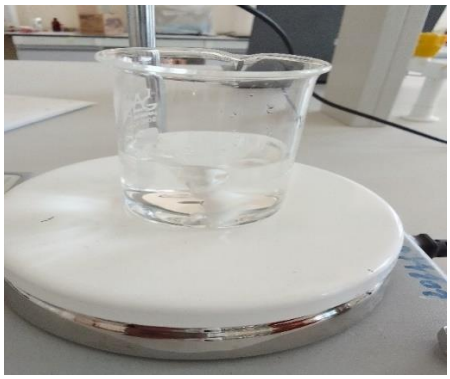

Figure 2: Solution B

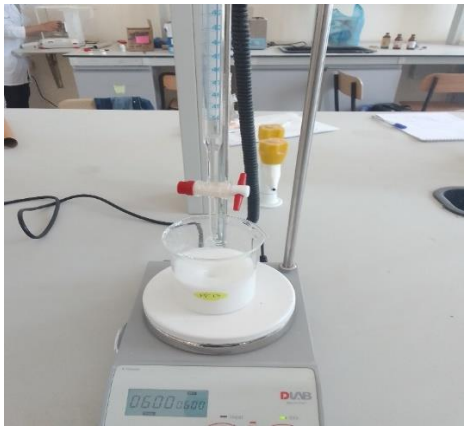

Figure 3: Solution B added drop by drop to A

Figure 4: Precipitation for two days

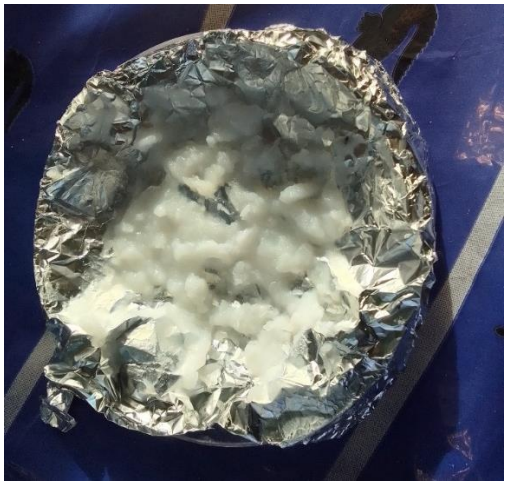

Figure 5: Drying

Figure 6: grind by pestle

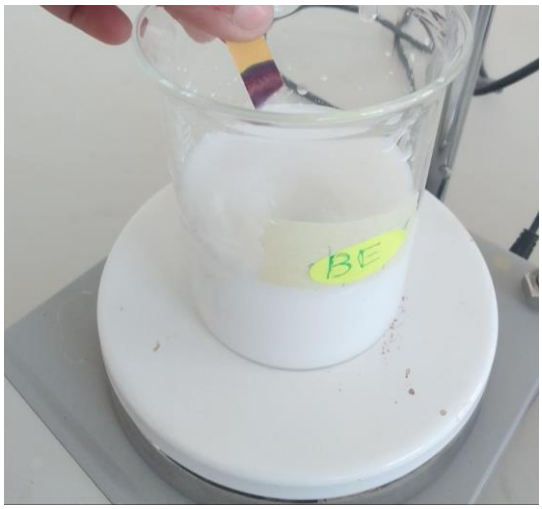

Figure 7: The synthesis of HAp by hydrothermal method

Figure 8: Teflon autoclave

Figure 9: Preparing the organic phase

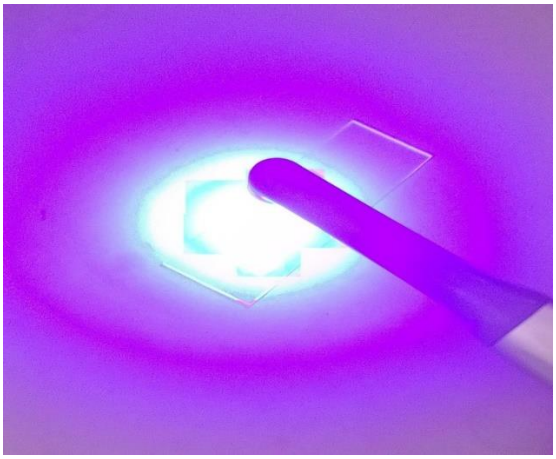

Figure 10: Visible lamp used in dental clinics

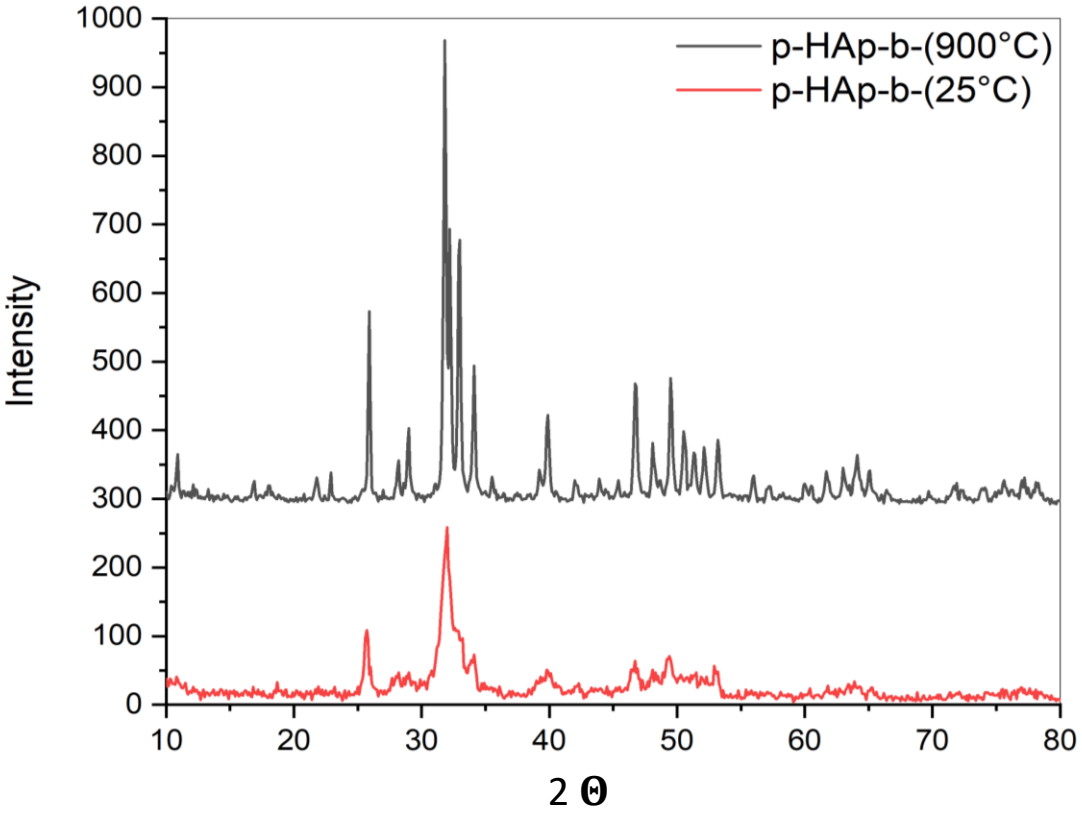

Figure 11: XRD patterns for p-HAp-b-(25°C), p-HAp-b-(900°C) powders.

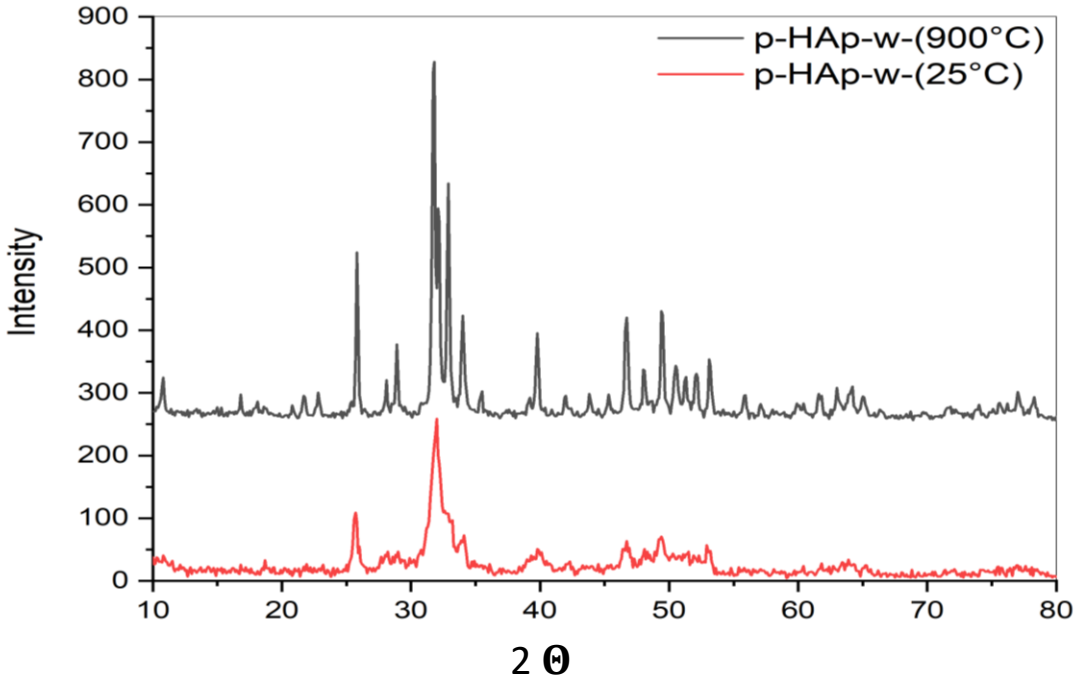

Figure 12: XRD patterns of p-HAp-w-(25°C), p-HAp-w-(900°C) powders.

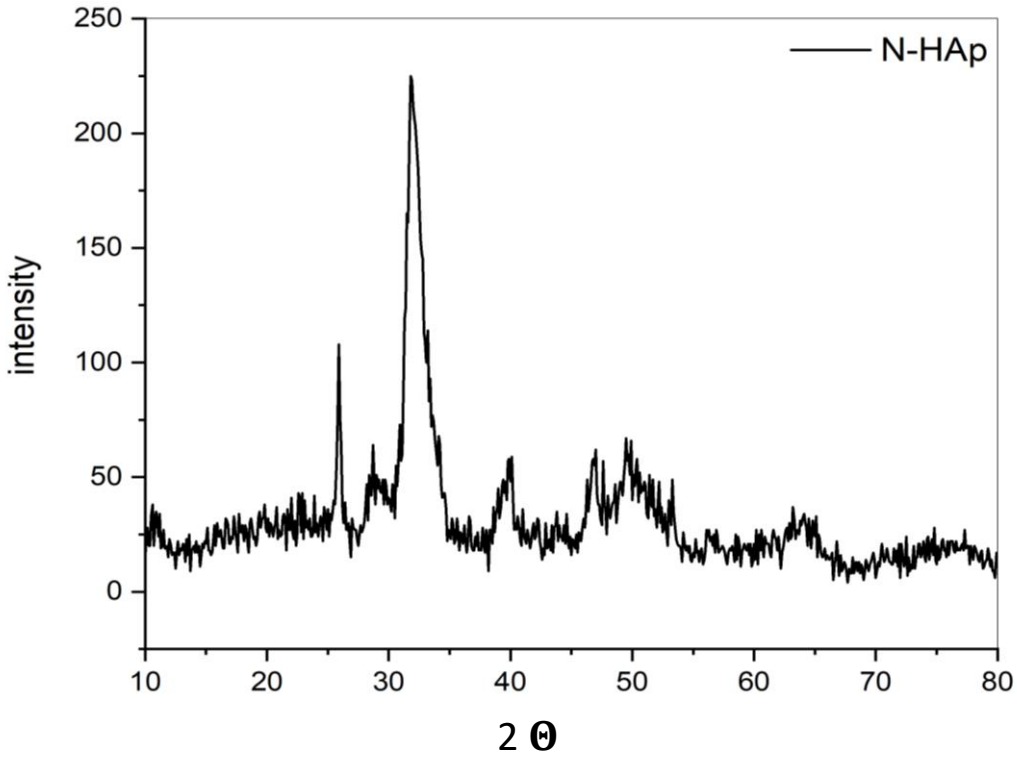

Figure 13: XRD patterns N-HAp powders.

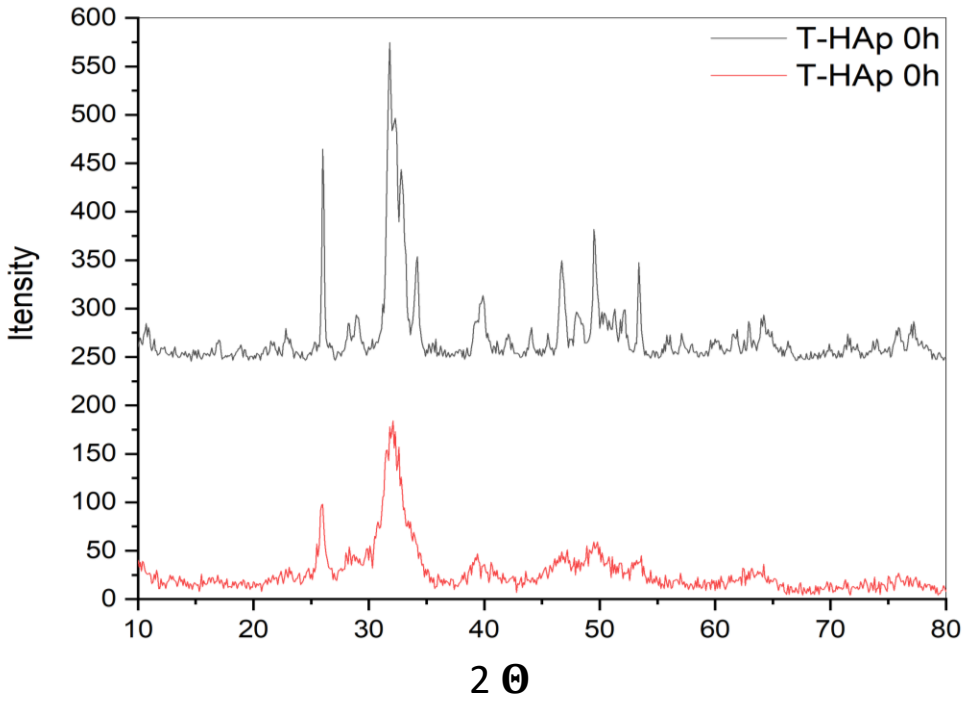

Figure 14: XRD patterns T-HAp 5h and T-HAp 5h powders.

Abstract:

Dentistry has recently witnessed a great development, by developing or replacing traditional methods with more advanced and safer methods for human health, including replacing amalgam with resin, because the amalgam contains toxic mercury. The resin prepared in our laboratory contains an organic phase consisting of TMPTMA as a monomer, DMAEMA as a catalyst, DEGDMA as a diluent, CQ as a photocatalyst and hydroxyapatite as a mineral phase. It is obtained in teflon autoclave for heat treatment, and we have adopted bovine bone as a natural source of hydroxyapatite. In order to know the best way to obtain hydroxyapatite closest to the natural source, FR-IR spectroscopy was used and the results were compared. The hydroxyapatite obtained from the two previous methods was taken and mixed in different proportions with the organic phase and exposed to visible light for photo-polymerization and resin formation. FR-IR spectroscopy was used, to find out the optimum ratios of each of the organic and metal phases to form the resin. X-rays were used to study the crystal structure of each of the hydroxyapatite obtained . To study the effect of polymerization time on the degree of polymerization, a mixture of organic phase and metal phase was exposed to different times of visible light and analyzed spectroscopically by FR-IR spectroscopy.

Key words: dental resin, Hydroxyapatite, photo-polymerization, teflon autoclave, chicken eggshells.

ملخص

شهد طب الأسنان في اللآونة الأخيرة تطورا كبيرا، و ذلك بتطوير أو بإستبدال طرق تقليدية لطرق أكثر تطورا و أمنا على صحة الإنسان، منها إستبدال الملغم بالراتنج و ذلك لإحتواء الملغم على مادة الزئبق السامة. يحتوي الراتنج المعد في مخبر من طور عضوي مكونة من TMPTMA كمونومير،DMAEMA كمحفز، DEGDMA كمخفف, CQ كمحفز ضوئي و hydroxyapatite كطور معدني تم تحضيره بطريقتين الأولى الترسيب التي أستخدم فيها قشور بيض دجاج كمصدر طبيعي للكالسيوم، و الثانية هي الطريقة الحرارية و ذلك بوضع hydroxyapatite المتحصل عليه في teflon autoclave لتلقي معاملة حرارية. إعتمد عظام البقر كمصدر طبيعي لل Hydroxyapatite . من أجل معرفة أفضل طريقة للحصول على hydroxyapatite الأقرب للمصدر الطبيعي. تم إستخدام مطيافية تحت الحمراء FR-IR وXRD و مقارنة النتائج المتحصل عليها. تم أخذ كل من ال hydroxyapatite المتحصل عليه من الطريقتين السابقتين و مزجه بنسب مختلفة مع الطور العضوي و تعريضها للضوء المرئي لحدوث بلمرة ضوئية و تشكيل الراتنج تم إستخدام التحليل الطيفي FR-IR ,لمعرفة النسب المثلى لكل من الطور العضوي و المعدني لتشكيل راتنج . لدراسة تأثير زمن البلمرة على درجة البلمرة تم تعريض مزيج من الطور العضوي إلى أزمنة مختلفة من ضوء المرئي و تحليلها طيفيا بواسطة مطيافية تحت الحمراء FR-IR . تم إستخدام الأشعة السينية لدراسة البنية الكريستالية لكل من hydroxyapatite المتحصل عليه من طريقة الترسيب بإستعمال بيض دجاج كمصدر للكالسيوم و المتحصل عليه بالطريقة الحرارية .

الكلمات المفتاحية : راتنج الأسنان, Hydroxyapatite, بلمرة الضوئية, Teflon autoclave, بيض الدجاج .